UNIVERSIDADE FEDERAL DO CEARÁ

***CAMPUS* SOBRAL**

PROGRAMA DE PÓS-GRADUAÇÃO EM ENGENHARIA ELÉTRICA E DE COMPUTAÇÃO

JUNO VITORINO SARAIVA

QOS-CONSTRAINED RADIO RESOURCE ALLOCATION ON OFDMA COOPERATIVE NETWORKS AND ON ENERGY-HARVESTING-AIDED MASSIVE MIMO SYSTEMS

SOBRAL

2019

JUNO VITORINO SARAIVA

QOS-CONSTRAINED RADIO RESOURCE ALLOCATION ON OFDMA COOPERATIVE NETWORKS AND ON ENERGY-HARVESTING-AIDED MASSIVE MIMO SYSTEMS

Dissertação apresentada ao Programa de Pós-Graduação em Engenharia Elétrica e de Computação do *campus* Sobral da Universidade Federal do Ceará, como requisito parcial à obtenção do título de mestre em Engenharia Elétrica e de Computação. Área de Concentração: Engenharia de Computação

Orientador: Prof. Dr. Francisco Rafael Marques Lima

SOBRAL

2019

Dados Internacionais de Catalogação na Publicação
Universidade Federal do Ceará
Sistema de Bibliotecas
Gerada automaticamente pelo módulo Catalog, mediante os dados fornecidos pelo(a) autor(a)

S246q Saraiva, Juno Vitorino.
QOS-CONSTRAINED RADIO RESOURCE ALLOCATION ON OFDMA COOPERATIVE NETWORKS AND ON ENERGY-HARVESTING-AIDED MASSIVE MIMO SYSTEMS / Juno Vitorino Saraiva. – 2019.
76 f. : il. color.

Dissertação (mestrado) – Universidade Federal do Ceará, Campus de Sobral, Programa de Pós-Graduação em Engenharia Elétrica e de Computação, Sobral, 2019.
Orientação: Prof. Dr. Francisco Rafael Marques Lima.

1. Radio resource allocation. 2. Quality of service. 3. Cooperative networks. 4. Energy efficiency. 5. Max-min fairness. I. Título.

CDD 621.3

To my parents.

AGRADECIMENTOS

First of all, I would like to thank my parents. Thank you very much, Mom and Dad, for always being there for me. I am deeply and sincerely grateful for everything you have done for me, and I will be eternally thankful.

I would also like to thank all my professors at UFC-Sobral for their valuable teachings. A very special thanks goes to my advisor, Prof. Dr. Rafael Lima, who has believed in me since I was an undergraduate student. Thank you very much, Prof. Dr. Rafael Lima, for your excellent supervision, support, encouragement, patience, and especially for believing in me.

In this context, I would like to express my most sincere gratitude to Prof. Dr. Rodrigo Cavalcanti and Prof. Dr. Tarcisio Maciel, who, together with Prof. Dr. Rafael Lima, gave me the opportunity to join the GTEL projects. It has been an enriching experience, both professionally and personally, to be part of this group. I am also thankful to all the personnel at the GTEL laboratory for their warm reception and pleasant coexistence.

Finally, I acknowledge the technical and financial support from CAPES, Ericsson Research, Wireless Access Network Department - Sweden, and Ericsson Innovation Center, Brazil, under the EDB/UFC.47 Technical Cooperation Contract.

"Your visions will become clear only when you can look into your own heart. Who looks outside, dreams; who looks inside, awakes."

(Carl Gustav Jung)

RESUMO

Nesta dissertação de mestrado, primeiramente estudamos a alocação de recursos de rádio (RRA, do inglês *radio resource allocation*) em redes cooperativas com a presença de múltiplos relays e múltiplos nós de destino, empregando OFDMA (*orthogonal frequency-division multiple access*). O RRA contempla o pareamento e o assinalamento de subportadoras, a seleção de relays e também a alocação de potência transmitida. Em detalhes, investigamos o impacto da qualidade de serviço (QoS, do inglês *quality of service*) ao maximizar a eficiência energética (EE, do inglês *energy efficiency*). Os três problemas estudados são: minimização da potência total de transmissão, maximização da EE total, e a maximização da mínima EE individual entre todos os nós de destino. Este último problema é capaz de oferecer justiça ao sistema em termos de EE. Em todos os três problemas, assumimos restrições de QoS. Apesar de alguns desses problemas serem fracionários e não lineares, fornecemos soluções ótimas usando algoritmos iterativos baseados na teoria da programação fracionária e programação fracionária generalizada. Além disso, apresentamos e demonstramos uma interessante propriedade que explora o uso do protocolo decodifica e encaminha (DF, do inglês *decode and forward*) presente nos relays deste trabalho, e mostramos como essa propriedade pode ser aplicada aos três problemas abordados, a fim de simplificá-los. Com isso, conseguimos reduzir consideravelmente o número de variáveis e restrições desses problemas e, consequentemente, reduzir suas complexidades computacionais. Finalmente, através de simulações computacionais, estudamos o desempenho das soluções fornecidas em termos de EE total, justiça de EE e QoS.

Parte desta dissertação também é dedicada a investigar a alocação de potência transmitida em sistemas MIMO massivo distribuídos auxiliados por colheita de energia (EH, do inglês *energy harvesting*). Em nosso modelo, o sistema MIMO massivo é representado por um conjunto muito grande de antenas distribuídas aleatoriamente ao longo de uma determinada área. Cada antena está acoplada a um ponto de acesso de energia híbrida (H-AP, do inglês *hybrid energy access point*), que simultaneamente serve a um número muito menor de usuários, cada um com uma única antena, sobre os mesmos recursos de tempo e frequência. Um H-AP consiste em APs (do inglês, *access points*) que são energizados tanto por uma fonte independente de energia renovável quanto por energia convencional da rede elétrica. O uso da rede elétrica compensa a intermitência e a aleatoriedade das fontes renováveis e permite garantias de QoS. Em cenários offline, onde se assume o conhecimento prévio da energia colhida (não causal), investigamos particularmente o problema de justiça max-min, maximizando a mínima razão sinal-interferência do sistema

(SINR, do inglês *signal to interference-plus-noise ratio*), considerando também requisitos de QoS. Também modelamos uma restrição em que o operador do sistema pode controlar a quantidade de energia consumida da rede elétrica e das fontes renováveis. Dado que o problema formulado tem natureza fracionária, garantimos sua solução ótima usando novamente a teoria da programação fracionária generalizada. No entanto, aqui também fornecemos uma abordagem alternativa para resolver de maneira ótima esse mesmo problema. Através de resultados numéricos, mostramos que, no cenário simulado, a solução alternativa é capaz de apresentar uma perda de desempenho em relação à solução ótima de apenas $10^{-1}\%$ quando configurada com 10 iterações. Além disso, essa solução alternativa também é capaz de acelerar o algoritmo generalizado de Dinkelbach e oferecer um interessante compromisso entre consumo de energia e perda de desempenho em relação à solução ótima. Por fim, discutimos o impacto das variáveis do problema sobre o desempenho do sistema.

Palavras-chave: Alocação de recursos de rádio; Qualidade de serviço; Redes cooperativas; Múltiplos *relays*; Eficiência energética; Justiça max-min; Teoria da programação fracionária e programação fracionária generalizada; MIMO massivo; Colheita de energia.

ABSTRACT

In this master's thesis, we first study radio resource allocation (RRA) for cooperative networks with multiple relays and destination nodes employing orthogonal frequency-division multiple access (OFDMA). RRA in our scenario includes relay selection, subcarrier pairing, and assignment, as well as transmit power allocation. Specifically, we analyze the impact of quality of service (QoS) when maximizing energy efficiency (EE). Three different problems are addressed in the first part of this work: total EE maximization, total power minimization, and minimum individual EE maximization. The last problem ensures fairness in the system regarding EE. In all three problems, we assume QoS constraints at the destination nodes. Although some of these problems are fractional and non-linear, we provide optimal solutions using iterative algorithms based on the theory of fractional programming and generalized fractional programming. Furthermore, we present and demonstrate an interesting property that exploits the use of the decode and forward (DF) protocol in the relay, and we show how it can be applied in the three problems discussed to simplify them. As a result, we can significantly reduce the number of variables and constraints in these problems, thereby reducing their computational complexity. Finally, through simulation results, we evaluate the performance of the proposed solutions in terms of total EE, EE fairness, and QoS.

Part of this master's thesis is dedicated to investigating transmit power allocation in an energy harvesting (EH)-aided distributed massive multiple input multiple output (MIMO) system. This distributed massive MIMO system involves a random distribution of a large number of single-antenna hybrid energy access points (H-APs) that simultaneously serve a much smaller number of single-antenna users over the same time/frequency resources. Additionally, we consider that each H-AP is powered by both an independent EH source and the electrical grid. The use of the electrical grid compensates for the intermittency and randomness of EH sources and allows for the provision of QoS guarantees. In offline scenarios, where prior knowledge of the EH profile is assumed (non-causal), we specifically investigate the max-min fairness problem by maximizing the minimum system signal-to-interference-plus-noise ratio (SINR) while fulfilling QoS requirements. We also model a problem constraint that allows the system operator to control the amount of energy consumed from the grid and renewable sources. Given that the formulated problem has a fractional framework, we guarantee its optimal solution by re-employing the theory of generalized fractional programming. However, we also provide an alternative approach to solve this problem optimally. Through numerical results, we show that in the simulated

scenario, the alternative solution presents a performance loss of only $10^{-1}\%$ compared to the optimal solution when configured for 10 iterations. Moreover, it also accelerates the convergence of the generalized Dinkelbach algorithm and offers an interesting trade-off between energy consumption and performance loss relative to the optimal solution. Lastly, we discuss the impact of the problem variables on system performance.

Keywords: Radio resource allocation; Quality of service; Cooperative networks; Multiple relays; Energy efficiency; Max-min fairness; Theory of fractional programming and generalized fractional programming; Massive MIMO; Energy harvesting.

LISTA DE ILUSTRAÇÕES

LISTA DE TABELAS

LIST OF ABBREVIATIONS AND ACRONYMS

3GPP	3rd generation partnership project
4G	4th generation
5G	5th generation
AF	amplify and forward
AWGN	additive white Gaussian noise
BB	branch and bound
BS	base station
CSI	channel state information
DF	decode and forward
EE	energy efficiency
EH	energy harvesting
FDM	frequency division multiplexing
FFT	fast fourier transform
H-AP	hybrid energy access point
ICT	information and communication technologies
IFFT	inverse fast fourier transform
ILP	integer linear problem
ITU	international telecommunications union
LP	linear programming
MCS	modulation and coding scheme
MIMO	multiple input multiple output
MISO	multiple input single output
MRT	maximum ratio transmission
MU-MIMO	multiuser MIMO
NOMA	nonorthogonal multiple access
OFDM	orthogonal frequency division multiplexing
OFDMA	orthogonal frequency division multiple access
OPEX	operational expenditures
PAPR	peak-to-average-power-ratio
QoS	quality of service
RRA	radio resource allocation

SINR	signal to interference-plus-noise ratio
SNR	signal-to-noise ratio
TTI	transmission time interval

SUMÁRIO

1 INTRODUCTION

This is an introductory chapter where we present the motivation and scope of this master's thesis in Section 1.1. After that, we present basic concepts and background about relevant topics to this thesis in Section 1.2, while the state of the art is reviewed in Section 1.3. Our main contributions and thesis organization are depicted in Section 1.4. Finally, the scientific production during the master's course is presented in Section 1.5.

1.1 Thesis Scope and Motivation

The exponential increase of data traffic and number of devices in mobile networks has led to an intense use of radio resources such as transmit power and frequency chunks. Particularly, the increase in transmit power leads to an intense energy consumption. Indeed, the increased demand for radio resources has become a growing concern since it is expected that the demand for wireless throughput, both mobile and fixed, is continuously increasing. According to Ericsson in (Ericsson, 2019), in the fourth quarter of 2018 the total number of mobile subscriptions was around 7.9 billion and the monthly mobile data traffic grew close to 88% between the fourth quarters of 2017 and 2018. Meanwhile, in (Gelenbe; Caseau, 2015) and (Consortium *et al.*, 2013), it was reported that almost 5% of the global energy is consumed by information and communication technologies (ICT) industry. Furthermore, ICT industry releases approximately 2% of the total CO_2 into the atmosphere, which currently is considered as a major threat for the environment. Although the previous CO_2 emission percentage may seem small, due to the advent of the 5th generation (5G) cellular mobile communications in the coming years, these statistics are expected to increase further and this can contribute to a sharp growth of energy consumption and greenhouse emission, besides billions of dollars spent on electricity.

A promising solution to these issues lies in optimizing the energy efficiency (EE) of ICT systems, which can be defined as the ratio between the system throughput and the corresponding energy consumed. Energy efficient ICT systems can be not only environment-friendly but also can achieve great financial savings by reducing operational costs. As a result, the concept of EE is nowadays an important performance metric when designing such systems and, therefore, improving EE of ICT systems becomes essential for the future of wireless communications. As stated by international telecommunications union (ITU) in its report (ITU-R Rec. M.2083, 2015), one of the 5G requirements is to increase the EE by 100 times and,

consequently, research towards designing energy-aware architectures has drawn extensive interest in the existing literature (Singh *et al.*, 2017).

Current ICT systems are predominantly powered by traditional carbon-based energy sources and using renewable energy, i.e., drawing energy from the environment, is particularly appealing as it theoretically constitutes an everlasting energy source. Furthermore, given that renewable energy is generally clean and cheap, it can reduce the carbon footprint and can reduce substantially the operational expenditures (OPEX) of the service providers. Thus, driven by environmental concerns, EH can be a promising technique towards green communications. Consequently, the goal is that ICT systems should not only be energy efficient when providing service coverage, but should also be self-sustainable. Nevertheless, the harvested energy is in general random in nature and the introduction of EH capabilities for ICT systems poses many new challenges for radio resource allocation (RRA) algorithm design (Jangsher *et al.*, 2015).

In this context, cooperative networks and distributed massive MIMO systems have also received significant attention since these technologies are the basis of the 4th generation (4G) and 5G networks, respectively (Li *et al.*, 2011; Ngo *et al.*, 2017). Both technologies also present a huge potential to meet the EE required by modern networks. However, both technologies also add a higher complexity to the network because of the increased flexibility in radio resource management. As examples, cooperative networks allow the selection of the most suitable relay to forward information while massive MIMO provides huge multiplexing gains. Moreover, quality of service (QoS) fulfillment and fairness are other objectives that can be optimized through RRA (Huaizhou *et al.*, 2014).

Motivated by this, in this master's thesis we focus on RRA problems that cover QoS fulfillment in cooperative networks and EH-aided distributed massive MIMO systems. Objectives such as fairness provision and EE maximization are studied.

1.2 Background

This section is devoted to the introduction of basic concepts that are relevant for the remaining of this thesis. In the following sections we introduce the orthogonal frequency division multiplexing (OFDM) and its multiple access method orthogonal frequency division multiple access (OFDMA), RRA, cooperative networks, massive MIMO systems and EH communications.

1.2.1 OFDM and OFDMA

OFDM and OFDMA are the modulation technique and the multiple access strategy adopted in the current 4G. Basically, OFDMA is an extension of OFDM and works as a multi-access technique by allocating different groups of orthogonal subcarriers to distinct terminals. In turn, OFDM emerged as an evolution of the traditional frequency division multiplexing (FDM) technique and it was initially proposed in 1968 (Chang; Gibby, 1968).

OFDM consists of the parallel transmission of data in several narrow band subcarriers in which the data rate per subcarrier is decreased as the number of subcarriers is augmented. Decreasing the data rate per subcarrier makes the system more robust to frequency-selectivity. Thus, working with narrow channels rather than a single wideband channel makes the system more immune to channel effects.

The main characteristic of OFDM is the use of precisely spaced subcarriers so that they are mathematically orthogonal. This generates spectral overlap and ensures significant bandwidth savings. Even with spectral overlap, the information driven by each of these subcarriers can be separated according to the scheme shown in Figure 1. As it can be seen, generation and reception of OFDM signals can be done employing inverse fast fourier transform (IFFT) and fast fourier transform (FFT) algorithms, respectively. A guard interval is used as a way to eliminate intersymbol interference which is very damaging for the received OFDM symbols. Moreover, the guard interval as a cyclic prefix keeps the orthogonal subcarriers even with the channel effects. According to this, the reception for OFDM symbols requires simple equalization. Therefore, in OFDM, the benefits of the use of a cyclic prefix are twofold: mitigate intersymbol interference (as a guard time) and avoid the interference among subcarriers (keeping them orthogonal at reception). However, although the cyclic prefix brings all these advantages and robustness to the OFDM, it is an overhead signal since it is a redundant information that wastes bandwidth and energy (Browning *et al.*, 2017).

Other problems even more serious such as high peak-to-average-power-ratio (PAPR) are present in OFDM systems, but this problem is not exclusive for OFDM and, therefore, it is present in any other multi-carrier modulation. In addition, it is possible to use simple and efficient techniques to reduce PAPR in OFDM systems in order to significantly improve signal quality. However, OFDM systems are quite sensitive to frequency deviations since the pulse shaping has high out-of-band emission. In general, this may not be important at high frequencies where large amount of bandwidth is available (Zaidi *et al.*, 2016).

Figura 1 – A simple OFDM transmission sketch.

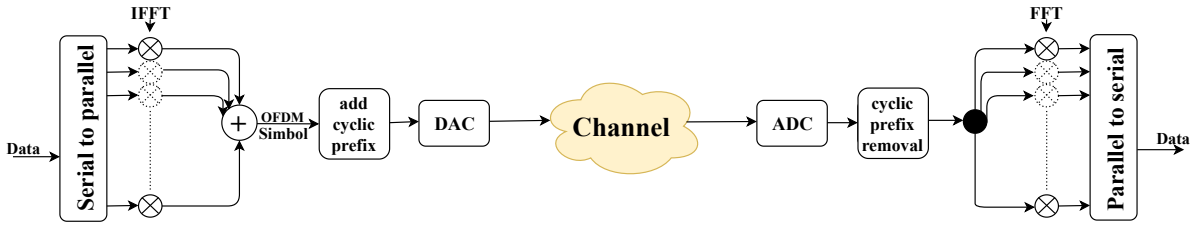

Fonte: (Gross; Bohge, 2006), adapted.

OFDM is widely employed nowadays and for 5G, 3rd generation partnership project (3GPP) has chosen the OFDM waveform from several waveform proposals (Zaidi *et al.*, 2016). This is because OFDM has some advantages that are appealing for future mobile networks. These advantages include high spectral efficiency despite the use of the cyclic prefix, high compatibility with MIMO systems, which allows to further increase spectral efficiency and coverage area, low implementation complexity and simple equalization process as discussed above. In addition, OFDM has robustness to channel frequency-selectivity, robustness to channel time-selectivity, flexibility, scalability, among others (Zaidi *et al.*, 2016).

1.2.2 Radio Resource Allocation

The rapid increase of the number of connected devices and the demands for high-speed multimedia communications stand in clear contrast to the rather limited radio resources. In this scenario, a possible solution is to use the scarce available radio resources in an efficient way by providing intelligent RRA algorithms and frameworks. Basically, RRA is responsible for the management of the system resources in the radio access networks with diverse objectives such as spectral and/or energy efficiences maximization and constraints such as fairness and QoS. (Chen *et al.*, 2012). We have been successfully applied to manage the resources of mobile networks along several generations and we do believe that it will still play a relevant role in modern networks.

Moreover, mobile networks need to face several other challenges that necessarily require well planned RRA designs. During the handover process, for example, resources should be allocated or reserved in advance in order to maintain connection or certain QoS requirements for a given terminal, i.e., an effective resource management should be required to ensure the success of the operation. When QoS constraints are concerned, some terminals may have a

higher priority when receiving radio resources for their transmission/reception. For example, the prioritization can be given for example to terminals due to the use of multimedia services that do not tolerate outage or interruption, or given to users that pay high subscription prices to use mobile services (Chen *et al.*, 2012). As the number of provided services and/or subscription classes increases, the efficient use of radio resource becomes more challeging and intelligent RRA solution are even more relevant.

Therefore, RRA plays a significant role in mobile networks since it defines mechanisms and procedures to share radio resource such as power, bandwidth, handover criteria, time slots, among others, in order to employ them as efficiently as possible.

1.2.3 Cooperative Networks

One of the biggest challenges of mobile networks is how to provide robust communication over fading channel. An interesting way to achieve this and, therefore, to mitigate the effects of fading is the use of diversity. In this context, cooperative networks can be an efficient an efficient solution since its main idea is to create multiple independent fading communication paths between the source and the destination. In this manner, relay-based cooperation can achieve diversity gains and, consequently, coverage, spectral efficiency and EE can be improved as well (Ng; Yu, 2007).

The simplest cooperative network occurs when there is a base station (BS), a terminal, and a device called relay that is capable of forwarding information from the BS to the terminal through an alternative channel. In this way, cooperative networks guarantee at least two independent and hopefully ucorrelated paths from the BS to the terminal that will receive two copies of the same signal. Using different paths for communication between BS and terminal is a powerful technique to mitigate fading and improve robustness to interference (Zhao *et al.*, 2006). Thereby, cooperative networks exploit the diversity inherent in multiple spatially distributed wireless links so that the diversity gains obtained are as high as the number of relays employed in the system. This type of diversity is known as cooperative diversity and, roughly speaking, occurs when several nodes, each with one or more antennas, form a kind of “coalition” to cooperatively act as a large transmit or receive array similarly to MIMO systems (Host-Madsen; Zhang, 2005).

Diferent benefits can be achieved through the efficient management of the relays due to the assumption of independence among the different paths. These benefits include improved reliability in data rate transmission, increased coverage area and also power savings. However,

the increasing number of relays comes at the cost of RRA solutions with a higher computational complexity and a significant burden in control signalling (Li *et al.*, 2011).

Relays can resort to different techniques when forwarding information signals from source node to the destinations. The two protocols most commonly used in cooperative communication are the amplify and forward (AF), which amplifies the received signal first, then broadcast it to the terminal, and the decode and forward (DF), which decodes the received signal to remove the noise before transmitting a clean copy of the original signal to the terminal. Thus, DF protocol requires more processing capacity since the signals have to be decoded at the relays and then forwarded. Nevertheless, unlike AF, the DF protocol does not propagate channel distortion and noise when the signal is correctly decoded at the relays (Host-Madsen; Zhang, 2005).

1.2.4 Massive MIMO systems

Increasing the capacity and reliability of wireless communication systems through the use of multiple antennas has been an unceasing area of research during the last two decades. Indeed, it has been shown in the literature that employing multiple antennas in both transmitter and receiver has potential to remarkably improve performance in terms of spectral efficiency, reliability and also EE. This type of technology emerged in the late 1990s and seminal works in this area focused primarily on point-to-point MIMO which represents the simplest form of MIMO systems. In this MIMO configuration, two devices with multiple antennas communicate with each other, e.g., a BS equipped with an antenna array serves a terminal also equipped with an antenna array. However, the actual implementation of multiple antennas in mobile terminals faces many drawbacks. Among the main issues we can mention the limited physical size and low-cost requirement for these terminals (Lu *et al.*, 2014; Marzetta; Yang, 2016).

As a result, in recent years the researchers have shifted the focus to multiuser MIMO (MU-MIMO) systems where several single antenna terminals are simultaneously served by a multiple-antenna BS. In other words, the MU-MIMO system is obtained from single antenna terminals by assuming that they compose a single virtual multiple-antenna terminal where the same multiplexing gains can be obtained (Lu *et al.*, 2014). Note that this is an important advantage of MU-MIMO over point-to-point MIMO configuration since high processing capacity requirement is kept on the BS side and, therefore, the terminals can be maintained relatively cheap in the single-antenna configuration. Furthermore, the performance of MU-MIMO is much

less sensitive to spatial correlation since in MU-MIMO different paths are in general independent among themselves, the so called multi-user diversity. Nevertheless, similar to point-to-point MIMO, MU-MIMO is not a scalable technology and the corresponding improvements owing to the employment of a high number of antennas are still modest. Fundamentally, this is because both point-to-point MIMO and MU-MIMO require the acquisition of channel state information (CSI) which can be obtained by means of pilot overhead (Marzetta; Yang, 2016).

Therefore, with the purpose of showing the true potential of MIMO systems, the massive MIMO concept was proposed by Marzetta in (Marzetta, 2010). Basically, the idea in that work was to propose an MU-MIMO where the number of antennas at BS is much larger than the number of served terminals. Thereby, it was shown that as the number of antennas at the transmitter grows without limit, all effects of uncorrelated noise and fast fading disappear and it makes simple linear processing nearly optimal. Furthermore, in massive MIMO only the BS obtains CSI and to acquire it, depending on the operating mode, the amount of resources required does not depend on the number of antennas at BS. All this stands out from traditional MU-MIMO and makes massive MIMO entirely scalable with respect to the number of antennas at BS (Marzetta; Yang, 2016). In summary, massive MIMO is an interesting and useful particular case of MU-MIMO and the main advantages of it includes huge spectral efficiency, high communication reliability, high energy efficiency and simple signal processing (Marzetta; Yang, 2016; Ngo, 2015). However, due to limited number of orthogonal pilots, the reuse of them in multicellular networks may be necessary causing a type of interference that significantly damages the system performance. This phenomenon is known as pilot contamination which, unlike other sources of interferences, does not vanish with unlimited number of antennas (Marzetta, 2010).

1.2.5 EH Communications

Traditionally, QoS constraints and spectral efficiency have been the predominant focus for the mobile network design (Ahmed *et al.*, 2015). However, as mobile networks are also commonly powered using batteries, energy can become a severe bottleneck and, thereby, prolonging the lifetime of a wireless network through EH communications has received significant attention recently (Nasir *et al.*, 2013). Besides, energy consumption has been a constant concern of modern mobile networks and employing EH communications in this sense can be quite promising for the future of wireless networks. EH comnunications can be defined as any system which draws part or all of its energy from the environment, i.e., nature or man-made

phenomena (Ulukus *et al.*, 2015). Various types of energy sources can be utilized to supplement energy supplies such as solar, wind, vibration, thermal, chemical, biological, indoor lighting, electromagnetic wave, among others. In addition, energy may also be harvested from man-made sources via wireless energy transfer, where energy is transferred from one node to another in a controlled manner (Ku *et al.*, 2015).

Employing EH communications in wireless systems can bring many promising advantages, including nearly permanent network lifetime and untethered mobility by breaking away from conventional battery recharging. Moreover, EH communications can lead to mainly reduction of carbon footprint and self-sustainability which is a crucial step in building next generation green and self-sufficient communication systems (Tutuncuoglu; Yener, 2012). Consequently, EH communications lead to a new paradigm shift of energy supply by decreasing the use of fossil fuels since its main idea is to generate energy from the sources which do not cause CO_2 emissions.

EH models play vital roles in designing energy scheduling and evaluating the performance of EH communications. Based on the availability knowledge about energy arrivals at the transmitters, the EH communications scenarios can be grouped into two types: offline and online optimization frameworks. In the offline optimization framework, it is assumed that the transmitter has non-causal information on the exact energy and data arrival instants and amount. Moreover, in this case, at the beginning of transmission, it is also considered full knowledge of CSI. On the other hand, in the online optimization framework, the transmitter is assumed to know the statistics of the underlying harvested energy and data arrival processes and has causal information about their realizations as well as CSI (Blasco *et al.*, 2013). As a result, EH models can bring new dimensions to the wireless network problem in the form of intermittency and randomness of harvested energy and, consequently, its optimization may require more effort for designing efficient RRA algorithms (Ulukus *et al.*, 2015). Furthermore, the harvested energy may also be scarce, requiring tailored transmission policies to achieve the desired performance (Tutuncuoglu; Yener, 2012). Thus, in order to ensure stringent QoS constraints and to compensate for the randomness of harvested energy, it is common for wireless networks to employ hybrid systems where the energy is supplied by both an energy harvester and a constant energy source, e.g., electrical grid.

1.3 State of the Art

The continuous evolution of wireless and mobile technologies depends fundamentally on efficient RRA strategies/schemes that are usually solutions of optimization problems composed of objective functions and constraint functions defined in a feasible domain. Due to its relevance, RRA has been extensively investigated in the literature. Thus, in this section, we highlight some works from the literature on RRA that have some similarity to the work developed in this thesis. Firstly, we review several works in the context of EE and fairness by considering different types of scenarios. Thus, this first of the literature review is related to the problems of Chapter 2 where we basically investigate EE and fairness in cooperative networks. Next, we cover works in the context of MIMO systems and EH communications which is related to the problem of Chapter 3.

Literature review related to Chapter 2

Depending on the purpose and characteristics of the mobile system, there are many different ways to measure EE (Chen *et al.*, 2010). Most commonly, EE can be defined as the ratio between the effectively transmitted data rate and the total expended power during the transmission process, including instantaneous and static components (Souza *et al.*, 2016). This type of EE metric that tries to find a balance between data rate and consumed power is common in the literature and can be found in many recent works such as (Masoudi *et al.*, 2018; D'Oro *et al.*, 2018; Yu *et al.*, 2016; Singh *et al.*, 2017; Wang *et al.*, 2018; Saraiva *et al.*, 2018). The maximization of the total system EE was considered in (Masoudi *et al.*, 2018) and (D'Oro *et al.*, 2018), while (Masoudi *et al.*, 2018) additionally assures QoS constraints to the terminals. A joint optimization problem of link-layer EE and effective capacity in a Nakagami-m fading channel under a delay-outage probability constraint and an average transmit power constraint was investigated in (Yu *et al.*, 2016). However, (Masoudi *et al.*, 2018), (D'Oro *et al.*, 2018) and (Yu *et al.*, 2016) did not consider a cooperative network. A utility-based joint subcarrier and power allocation algorithm for improving the EE in multi-destination two-way regenerative relay networks was investigated in (Singh *et al.*, 2017). The EE maximization for an OFDMA downlink network aided by a relay station with subcarrier pairing was studied in (Wang *et al.*, 2018). Although (Singh *et al.*, 2017) and (Wang *et al.*, 2018) considered cooperative networks, the problem complexity was reduced by assuming only one relay station. An RRA problem with

cooperative networks with multiple relays was addressed in (Saraiva *et al.*, 2018). Nevertheless, in (Saraiva *et al.*, 2018) the authors focused only on maximizing the total system EE while satisfying the minimum required data rate of all users. Therefore, similar to (Masoudi *et al.*, 2018; D'Oro *et al.*, 2018; Yu *et al.*, 2016; Wang *et al.*, 2018; Singh *et al.*, 2017), in (Saraiva *et al.*, 2018) other problem objectives, such as fairness in resource allocation, were not considered.

The provision of fairness in RRA has been considered in some works in the literature (Li *et al.*, 2015; Nguyen *et al.*, 2015; Sokun *et al.*, 2018; Singh; Chaturvedi, 2017; Song *et al.*, 2016; Sheng *et al.*, 2015). Max-min fairness guarantees in non-cooperative networks has been studied in (Li *et al.*, 2015; Nguyen *et al.*, 2015; Sokun *et al.*, 2018). Specifically, in (Li *et al.*, 2015) a max-min EE-optimal problem to ensure fairness among links in OFDMA systems was solved. In detail, the EE of the worst-case link subject to the rate requirements, transmit power, and subcarrier assignment constraints is maximized. The fairness in terms of achievable EE in a multicell multiuser multiple input single output (MISO) downlink system with a beamforming scheme to maximize the minimum EE among all BSs is investigated in (Nguyen *et al.*, 2015). The problem of optimizing resource allocation in uplink OFDMA networks for providing EE fairness among the users while considering discrete transmit power levels was addressed in (Sokun *et al.*, 2018). Particularly, the paper focused on how to maximize the minimum user EE in the network by jointly optimizing resource blocks and discrete power allocation, without considering QoS requirements.

In (Singh; Chaturvedi, 2017; Song *et al.*, 2016; Sheng *et al.*, 2015) fairness was studied in cooperative networks with multiple relays. In (Singh; Chaturvedi, 2017) the authors investigated a multi-user MIMO relay system, where several transmit nodes simultaneously communicate with their respective receive nodes through half duplex MIMO AF relay nodes. The problem was formulated as the maximization of the minimum SINR per stream among all the users subject to transmit power constraints at the transmitter and relay nodes. The trade-off among spectral efficiency, EE, and fairness in terms of data rate in cooperative OFDMA systems with DF relaying was studied in (Song *et al.*, 2016), where subcarrier pairing and assignment, relay selection, transmission strategy selection, and power allocation were jointly considered. The fairness in terms of data rate was represented using the $\alpha-$fairness model and the resource allocation problem was formulated as a multi-objective optimization problem. Therefore, unlike (Singh; Chaturvedi, 2017) and (Song *et al.*, 2016) we consider fairness in terms of EE. Lastly, an adaptive relay selection rule that can serve as an effective tool to achieve a desirable trade-off

between fairness and energy consumption was introduced in (Sheng *et al.*, 2015). Moreover, it was also proposed a power-allocation method to optimize the DF cooperative transmission for source and relay nodes as a means to reduce the total power consumption, while maintaining the required QoS. However, the considered EE metric consists only in the power consumption of network nodes and, therefore, it was not able to optimize the trade-off between transmit data rate and power consumption.

Literature review related to Chapter 3

Both massive MIMO and EH are well studied technologies that have been constantly investigated in the literature. In massive MIMO systems, several problems with different aims have been proposed such as max-min fairness, and the maximization of spectral efficiency and energy efficiency in an individual fashion or jointly in (Ngo *et al.*, 2017; Arash *et al.*, 2017; Hamdi; Ajib, 2015; Liu *et al.*, 2017; Hu *et al.*, 2014). Nevertheless, none of these articles considered the employment of EH communications. On the other hand, EH for single-antenna transceivers has been addressed in (Carvalho *et al.*, 2018; Ming *et al.*, 2015; Jiang *et al.*, 2015; Song; Xu, 2018). In (Carvalho *et al.*, 2018) an RRA problem was investigated where the aim is to maximize throughput in an OFDMA system considering also QoS constraints. In that work, the authors considered the case where the energy source is obtained solely from solar energy from photovoltaic panels and a hybrid case where energy comes from photovoltaic panels and from the grid. Differently of (Carvalho *et al.*, 2018), in (Ming *et al.*, 2015; Jiang *et al.*, 2015; Song; Xu, 2018) EH scenarios were addressed in cooperative networks. The purpose in (Ming *et al.*, 2015) was to propose a resource allocation scheme to maximize the energy efficiency of the system, where the relay was powered only by the harvested energy. On the other hand, the main objective in the articles (Jiang *et al.*, 2015) and (Song; Xu, 2018) was to investigate joint relay selection and power allocation schemes in order to maximize the system throughput assuming half-duplex and full-duplex relays, respectively. However, similar to (Ming *et al.*, 2015), (Jiang *et al.*, 2015) and (Song; Xu, 2018), the authors did not consider the hybrid case since the relay stations were powered only by EH sources. Although EH sources have many advantages, they present a stochastic nature and this might jeopardize service guarantees to users in more realistic scenarios. Therefore, a hybrid system design, which uses grid energy in a complementary manner, is preferable in practice for providing uninterrupted service.

Massive MIMO systems combined with EH technology can be found in (Hamdi *et*

al., 2017; Zhang *et al.*, 2018; Kuang *et al.*, 2017; Zhao; Zheng, 2016). In (Hamdi *et al.*, 2017) the authors investigated the energy consumption of distributed massive MIMO systems using hybrid energy. More specifically, a minimization problem of grid power consumption subject to QoS constraint per user was formulated, the optimal solution was found and a heuristic algorithm was provided. Both offline and online scenarios were considered in that paper. Similar to (Hamdi *et al.*, 2017), in (Zhang *et al.*, 2018) the authors also considered online and offline scenarios with hybrid EH BS, but the goal was the system throughput maximization without considering QoS constraints. However, neither (Hamdi *et al.*, 2017) nor (Zhang *et al.*, 2018) addressed fairness in their problem formulations. Motivated by this, fairness was taken into account in the studies presented in (Kuang *et al.*, 2017) and (Zhao; Zheng, 2016). Nevertheless, these articles did not consider QoS and focus on EH models based on wireless energy transfer technology, where utility functions were employed in order to achieve improved efficiency/fairness.

1.4 Thesis Organization and Contributions

In this section we present the organization of this master's thesis by describing each chapter in details in order to show our main contributions.

In Chapter 2, we investigate a cooperative network with multiple relays and multiple destination nodes. Basically, we investigate some relevant RRA problems in the form of non-convex optimization problems each one being composed of four subproblems: subcarrier pairing, relay selection, subcarrier assignment and transmit power allocation. Our goal is to study the impact of QoS on important problems within the EE and fairness context. The studied problems are total power minimization, total EE maximization and minimum individual EE maximization. The latter is able to ensure fairness in the resource allocation in terms of EE. All these problems are subject to QoS constraints and individual power constraints in each network node. Although some of these problems are fractional and non-linear, optimal solutions are provided by using iterative algorithms based on the theory of fractional programming and generalized fractional programming. Furthermore, we present and demonstrate an interesting property that exploits the employment of the DF protocol present in the relays and we show how it can be applied in the three problems addressed herein to simplify them. Thereby, we are able to considerably reduce the number of variables and constraints of these problems and, therefore, reducing their computational complexity. In addition, we assume that the mapping between signal-to-noise ratio (SNR) and transmit data rate is discrete so as to better model practical networks. This

assumption leads to important changes in both performance and problem solving and is rarely employed in the literature since taking this into account can make the optimization problems even harder. It is important to note that working in a cooperative network with multiple relays considering subcarrier pairing and assignment, relay selection and transmitted power allocation is rarely found in the literature. In addition, in this scenario we investigate three important problems in the context of EE and EE fairness and this is not considered in any work reviewed in Section 1.3.

In Chapter 3, we formulate an RRA problem in the context of massive MIMO communications with EH-capable nodes, in which the circuit energy consumption, the limited battery storage capacity, and minimum SINR requirements are taken into consideration. The considered system is composed of a large set of single-antenna H-APs that are uniformly distributed in the coverage area and each of them is powered by an independent EH source and the electrical grid, i.e., the grid energy is assumed as a complementary energy supplement to the system. The H-APs are responsible for transmitting data information to a number of users over the same time/frequency resources with the aim of providing fairness and satisfying their QoS demands. To be specific, our RRA problem is formulated as an optimization problem for optimizing the transmit power in order to provide max-min fairness in terms of SINR considering also QoS constraints in offline scenarios. The study of offline scenarios is considered important in the literature since it provides a bound on the performance of the corresponding online problem. To solve the formulated max-min fairness problem we employ concepts of generalized fractional programming and as well as an alternative approach to optimally solve the problem. Furthermore, motivated by environmental issues, we limit the grid energy consumption relative to the havested energy and discuss the effects of that consideration. In the results, we show the performance of both optimal solutions on the fairness-oriented resource allocation and we highlight some important trade-offs in the context of our problem. As discussed, massive MIMO and EH are widely studied subjects in the literature but few works exploit them together. Thus, we investigate a fairness problem that in the scenario considered in this thesis is not found in any work discussed in the state of the art of Section 1.3.

In Chapter 4, we conclude this thesis by summarizing and highlighting the main points of this thesis and we also point out the main research directions that can be considered as extension and future works.

1.5 Scientific Production

Part of the content and contributions of chapter 2 of this master's thesis were published with the following information:

- **Juno V. Saraiva**, Jair A. de Carvalho, F. Rafael M. Lima, Tarcisio F. Maciel and F. Rodrigo P. Cavalcanti, *"Alocação de Recursos em Sistemas Cooperativos para Maximização da Eficiência Energética Sujeita a Restrições de QoS"*. In: PROCEEDINGS of the Brazilian Telecommunications Symposium (SBrT). São Pedro, Brazil, 2017.
- **Juno V. Saraiva**, F. Rafael M. Lima, Tarcisio F. Maciel and F. Rodrigo P. Cavalcanti, *"Relay Selection, Subcarrier Pairing and Power Allocation for Energy Efficiency and QoS Guarantees"*. In: PROCEEDINGS of the IEEE Wireless Communications and Networking Conference (WCNC). Barcelona, Spain, 2018.

  Other works regarding chapters 2 and 3 are to be submitted.

- **Juno V. Saraiva**, F. Rafael M. Lima, Alexandre M. Pessoa, Tarcisio F. Maciel and F. Rodrigo P. Cavalcanti, *"QoS-Constrained Radio Resource Allocation for Energy Efficiency Optimization in Cooperative Networks."* [to be submitted to a journal].
- **Juno V. Saraiva**, F. Rafael M. Lima, Tarcisio F. Maciel and F. Rodrigo P. Cavalcanti, *"Max-Min Fairness in an Energy-Harvesting-Aided and QoS-Constrained Massive MIMO System."* [to be submitted to a journal].

Another research work that was performed during the master course and is not present in this thesis was published with the following information:

- Jair A. de Carvalho, **Juno V. Saraiva**, F. Rafael M. Lima, Tarcisio F. Maciel and F. Rodrigo P. Cavalcanti, *"Resource Allocation for OFDMA Systems and Energy Harvesting Communications in Multi-User Offline Scenarios"*. In: PROCEEDINGS of the Brazilian Telecommunications Symposium (SBrT). São Pedro, Brazil, 2017.

In parallel to the work developed in the master course that was initiated on the second semester of 2017, we have been working on other research projects related to machine learning for intelligent control of 5G networks. In the context of these projects, we have participated on the following works:

- **Juno V. Saraiva**, Victor F. Monteiro, F. Rafael M. Lima, Tarcisio. F. Maciel and F. Rodrigo P. Cavalcanti, *"A Q-learning Based Approach to Spectral Efficiency Maximization in Multiservice Wireless Systems"*. In: PROCEEDINGS of the Brazilian Telecommunications Symposium (SBrT). Petrópolis, Brazil, 2019 [submitted].

- Juno V. Saraiva, Victor F. Monteiro, Diego A. Sousa, Weskley V. F. Maurício, F. Rafael M. Lima, Tarcisio F. Maciel and F. Rodrigo P. Cavalcanti, *"Radio Resource Allocation and QoS Management in Multi-User, Multi-Service and Multi-RAT 5G Systems"*. GTEL-UFC-Ericsson UFC.47, Tech. Rep., April 2019, First Technical Report.

2 RADIO RESOURCE ALLOCATION FOR ENERGY EFFICIENCY OPTIMIZATION IN COOPERATIVE NETWORKS

2.1 Introduction

In this chapter, we investigate three RRA problems in the form of optimization problems involving cooperative networks with multiple relays and destination nodes. The studied problems include the total power minimization, total EE maximization and minimum individual EE maximization subject to QoS constraints and individual power constraints in each node of the network. This chapter is organized as follows. In Section 2.2 we present the assumed system modeling and scenario and define the main variables related to the three RRA problems. The mathematical formulations of these problems are shown in Section 2.3. In Sections 2.4 and 2.5 we present a simplification of the problems and their optimal solutions, respectively. Simulation results and discussions are provided in Section 2.6 and, finally, concluding remarks are given in Section 2.7.

2.2 Channel and System Modeling

We consider a communication system using OFDMA and having a transmitting source (BS, in our model), K relay nodes, and J destination nodes. Due to severe path loss and shadowing, we assume that the source and destination nodes are unable to communicate directly and, therefore, the relays are responsible for information forwarding. There are N orthogonal OFDMA subcarriers that can be commonly used in the source-relay hop (hop 1) and the relay-destination hop (hop 2). The relays operate in the half-duplex mode and the transmission of information occurs in two time slots, where in the first time slot, the source transmits information to the relays, and in the second one, the relays forward the information to the destination nodes. We assume $\mathcal{N} = \{1, \ldots, N\}$ as the set of all subcarriers, $\mathcal{K} = \{1, \ldots, K\}$ as the set of all relays, and $\mathcal{J} = \{1, \ldots, J\}$ as the set of all destination nodes. Information processing at the relay is done by the DF protocol. Thus, the relays first receive the information signal, perform detection and decoding, and finally re-encode information for transmission.

We assume as *subcarrier pairing* the process of defining for each subcarrier of hop 1, the corresponding subcarrier of hop 2 that will forward the information sent from the source. *Subcarrier assignment* consists in assigning a subcarrier q from hop 2 to a destination node j. In order to avoid possible interference between relays, each subcarrier of hops 1 and 2 can only be

Figura 2 – Communication system with a transmitter source, K relays and J destination nodes.

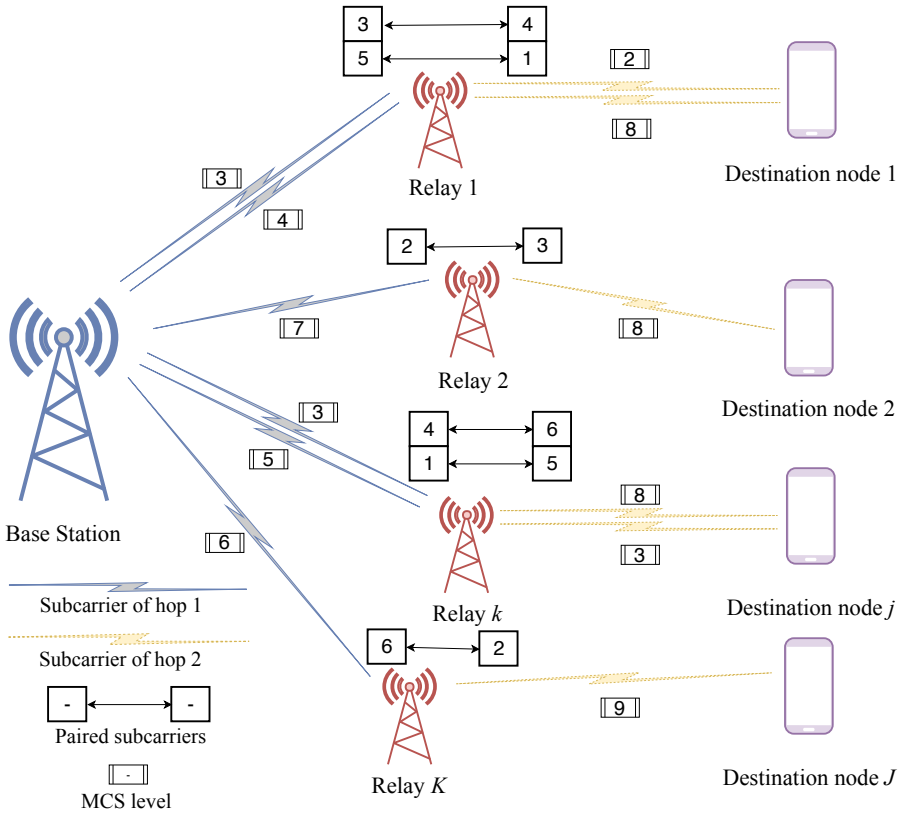

Fonte: Created by the author.

associated with a single relay during the half duplex transmission. Each relay, on the other hand, can make several simultaneous subcarrier pairings. The process of defining which relay will perform the pairing of two paired subcarriers is called *relay selection*. It is important to highlight that relay selection and subcarrier assignment problems are only present when multiple relays and multiple destination nodes are assumed, respectively. Few works presented in the literature review in Section 1.3 assumed multiple relays in the cooperative system.

The SNR $\gamma^{\mathrm{s}}_{n,k}$ of subcarrier n in hop 1 when associated with relay k, and the SNR $\gamma^{\mathrm{r}}_{q,k,j}$ of subcarrier q of hop 2 when associated with relay k and assigned to destination node j, are given respectively by

$$\gamma^{\mathrm{s}}_{n,k} = \frac{p^{\mathrm{s}}_{n} \cdot \alpha^{\mathrm{s}}_{k} \cdot |h^{\mathrm{s}}_{n,k}|^2}{\sigma^2}, \text{ and } \gamma^{\mathrm{r}}_{q,k,j} = \frac{p^{\mathrm{r}}_{q} \cdot \alpha^{\mathrm{r}}_{k,j} \cdot |h^{\mathrm{r}}_{q,k,j}|^2}{\sigma^2}, \tag{2.1}$$

where $|h^{\mathrm{s}}_{n,k}|$ and $|h^{\mathrm{r}}_{q,k,j}|$ represent the magnitude of the complex frequency response of subcarrier n of hop 1 when associated with relay k, and subcarrier q of hop 2 when associated with relay k and assigned to destination node j, respectively. p^{s}_{n} is the power allocated by the source to subcarrier n of hop 1 and p^{r}_{q} is the power allocated by relay k to subcarrier q of hop 2. σ^2 is the average power of the thermal noise and, finally, α^{s}_{k} and $\alpha^{\mathrm{r}}_{k,j}$ model the effect of long-term path

loss and shadowing of the links between source node and relay k in hop 1, and between relay k and destination node j in hop 2, respectively. We assume that $P^{\text{s}}_{\text{total}}$ is the total power available at source and that P^{k}_{total} is the total power available at relay k.

Tabela 1 – Mapping from SNR to transmit data rate per subcarrier.

Range of SNR	**Transmit data rate**
$\gamma^1 \leq (\gamma^{\text{s}}_{n,k}$ or $\gamma^{\text{r}}_{q,k,j}) < \gamma^2$	r_1
$\gamma^2 \leq (\gamma^{\text{s}}_{n,k}$ or $\gamma^{\text{r}}_{q,k,j}) < \gamma^3$	r_2
$\vdots$	$\vdots$
$\gamma^{M-1} \leq (\gamma^{\text{s}}_{n,k}$ or $\gamma^{\text{r}}_{q,k,j}) < \gamma^M$	r_{M-1}
$(\gamma^{\text{s}}_{n,k}$ or $\gamma^{\text{r}}_{q,k,j}) \geq \gamma^M$	r_M

Let $\varphi(\cdot)$ be the link adaptation function responsible for mapping the SNR to the transmit data rate on each subcarrier. This is a discrete and monotonic increasing function that models the modulation and coding scheme (MCS) levels in a practical wireless network. Thus, the data rate transmitted in a subcarrier n of hop 1 associated with relay k and in a subcarrier q of hop 2 associated with relay k and assigned to destination node j are given by $\varphi\left(\gamma^{\text{s}}_{n,k}\right)$ and $\varphi\left(\gamma^{\text{r}}_{q,k,j}\right)$, respectively.

We assume in this study M possible levels of MCS contained in the set $\mathcal{M} = \{1, \ldots, M\}$. We define as r_m the data rate when the m-th MCS level is used in a given subcarrier[1]. In order to have a transmission in the m-th MCS level with an acceptable bit error rate, it is required that the SNR of the subcarrier be equal to γ^m where $\gamma^{m+1} > \gamma^m$ as shown in Table 1. Thus, we define $p^{\text{s}}_{n,m,k}$ as the transmit power needed by subcarrier n of hop 1 associated with relay k in order to transmit at the m-th MCS level. Similarly, we define $p^{\text{r}}_{q,m,k,j}$ as the transmit power needed by subcarrier q of hop 2, associated with relay k and assigned to destination node j in order to transmit at the m-th MCS level. $p^{\text{s}}_{n,m,k}$ and $p^{\text{r}}_{q,m,k,j}$ can be calculated from (2.1) and $\varphi(\cdot)$.

The main aspects of our system modeling are illustrated in Figure 2. In relay 2, for example, the subcarriers 2 and 3 of hop 1 and hop 2, respectively, were paired, and destination node 2 is assigned. Furthermore, the 7-th and 8-th MCS levels were set to subcarriers 2 and 3, respectively. The same reasoning applies to any other relay present in Figure 2.

We define the optimization binary variables as $y^{\text{s}}_{n,m,k}$ and $y^{\text{r}}_{n,q,m,k,j}$, where $y^{\text{s}}_{n,m,k}$ assumes the value 1 when the source transmits at the m-th MCS level on subcarrier n of hop 1

[1] We consider that in the first MCS level ($m = 1$) we have $r_1 = 0$.

to the k-th relay, and 0 otherwise, and $y^{\mathrm{r}}_{n,q,m,k,j}$ assumes 1 when the k-th relay transmits at the m-th MCS level on subcarrier q of hop 2 that is paired with subcarrier n of hop 1 and assigned to destination node j, and 0 otherwise. Note that when $y^{\mathrm{s}}_{n,m,k} = 1$, the power allocated to subcarrier n is $p^{\mathrm{s}}_{n,m,k}$, whereas the transmit power in subcarrier q is $p^{\mathrm{r}}_{q,m,k,j}$ when $y^{\mathrm{r}}_{n,q,m,k,j} = 1$.

We define r^{s}_n as the transmit data rate in the n-th subcarrier of hop 1 and $r^{\mathrm{r}}_{n,q}$ as the transmit data rate in the q-th subcarrier of hop 2 that is paired with the n-th subcarrier of hop 1. We define *link* as the set of two paired subcarriers. Thus, the end-to-end data rate on the n-th link is given by $\min\left\{r^{\mathrm{s}}_n, r^{\mathrm{r}}_{n,q}\right\}$ due to the use of the DF protocol (Saraiva *et al.*, 2018; Silva *et al.*, 2012). Table. 2 summarizes the main variables defined in this section [2].

Tabela 2 – Summary of the main variables of chapter 2.

Variable	Description
N	Number of OFDMA subcarriers at each hop.
M	Number of MCS levels.
K	Number of relays.
J	Number of destination nodes.
$\mathcal{N}$	Set of all subcarriers.
$\mathcal{M}$	Set of all levels of MCS.
$\mathcal{K}$	Set of all relays.
$\mathcal{J}$	Set of all destination nodes.
$y^{\mathrm{s}}_{n,m,k}$	Optimization binary variable of hop 1. $y^{\mathrm{s}}_{n,m,k}$ assumes 1 when the source transmits at the m-th MCS level on subcarrier n of hop 1 to the k-th relay, and 0 otherwise.
$y^{\mathrm{r}}_{n,q,m,k,j}$	Optimization binary variable of hop 2. $y^{\mathrm{r}}_{n,q,m,k,j}$ assumes 1 when the k-th relay transmits at the m-th MCS level on subcarrier q of hop 2 that is paired with subcarrier n of hop 1 and assigned to destination node j, and 0 otherwise.
r_m	Data rate when the m-th MCS level is used in a given subcarrier.
r^{s}_n	Transmit data rate in the n-th subcarrier of hop 1.
$r^{\mathrm{r}}_{n,q}$	Transmit data rate in the q-th subcarrier of hop 2 that is paired with the n-th subcarrier of hop 1.
$P^{\mathrm{s}}_{\mathrm{total}}$	Total power available at source.
P^{k}_{total}	Total power available at relay k.
$p^{\mathrm{s}}_{n,m,k}$	Power allocated to subcarrier n of hop 1 when $y^{\mathrm{s}}_{n,m,k} = 1$.
$p^{\mathrm{r}}_{q,m,k,j}$	Power allocated to subcarrier q of hop 2 when $y^{\mathrm{r}}_{n,q,m,k,j} = 1$.

2.3 Problem Formulations

In this section, we present the mathematical formulation of total power minimization, total EE maximization and minimum individual EE maximization problems. We begin by stating the main system constraints that are common to the three problems. Firstly, each subcarrier n of hop 1 only transmits in a single MCS level and can only be associated with a single relay

[2] The variables defined in the Table 2 are valid only in this chapter.

according to (2.2a). In addition, each subcarrier q of hop 2 should transmit in a unique MCS level, be associated with a single relay node, be paired with a single subcarrier in hop 1 and, finally, be assigned to a single destination node. Similarly, each subcarrier n of hop 1 should be paired with a unique subcarrier in hop 2 that is assigned to a single relay transmitting in a given MCS level and associated with a single destination node. Both constraints are assured by equations (2.2b) and (2.2c). According to (2.2d), the pairing of two specific subcarriers of hops 1 and 2 should be performed by a single relay.

$$\sum_{m\in\mathcal{M}}\sum_{k\in\mathcal{K}} y^{\mathrm{s}}_{n,m,k} = 1, \quad \forall n \in \mathcal{N}, \tag{2.2a}$$

$$\sum_{n\in\mathcal{N}}\sum_{m\in\mathcal{M}}\sum_{k\in\mathcal{K}}\sum_{j\in\mathcal{J}} y^{\mathrm{r}}_{n,q,m,k,j} = 1, \quad \forall q \in \mathcal{N}, \tag{2.2b}$$

$$\sum_{q\in\mathcal{N}}\sum_{m\in\mathcal{M}}\sum_{k\in\mathcal{K}}\sum_{j\in\mathcal{J}} y^{\mathrm{r}}_{n,q,m,k,j} = 1, \quad \forall n \in \mathcal{N}, \tag{2.2c}$$

$$\sum_{m\in\mathcal{M}} y^{\mathrm{s}}_{n,m,k} - \sum_{q\in\mathcal{N}}\sum_{m\in\mathcal{M}}\sum_{j\in\mathcal{J}} y^{\mathrm{r}}_{n,q,m,k,j} = 0, \forall n \in \mathcal{N}, \forall k \in \mathcal{K} \tag{2.2d}$$

Constraints (2.3a) and (2.3b) guarantee that the total transmit power at source and each relay k should not be higher than the available power at source, P^{s}, and at each relay k, P^k, respectively. The total used power in the whole system is represented by (2.4). It is common in the literature to consider a single power constraint for all relays or for the entire system (see, e.g., (Song *et al.*, 2016)). While this is in practice unrealistic, it is used to simplify the structure of problems.

$$\sum_{n\in\mathcal{N}}\sum_{m\in\mathcal{M}}\sum_{k\in\mathcal{K}} y^{\mathrm{s}}_{n,m,k}\cdot p^{\mathrm{s}}_{n,m,k} \leq P^{\mathrm{s}}, \tag{2.3a}$$

$$\sum_{n,q\in\mathcal{N}}\sum_{m\in\mathcal{M}}\sum_{j\in\mathcal{J}} y^{\mathrm{r}}_{n,q,m,k,j}\cdot p^{\mathrm{r}}_{q,m,k,j} \leq P^k, \quad \forall k \in \mathcal{K}, \tag{2.3b}$$

$$P = \sum_{n\in\mathcal{N}}\sum_{m\in\mathcal{M}}\sum_{k\in\mathcal{K}} y^{\mathrm{s}}_{n,m,k}\cdot p^{\mathrm{s}}_{n,m,k} + \sum_{n,q\in\mathcal{N}}\sum_{m\in\mathcal{M}}\sum_{k\in\mathcal{K}}\sum_{j\in\mathcal{J}} y^{\mathrm{r}}_{n,q,m,k,j}\cdot p^{\mathrm{r}}_{q,m,k,j} + p_{\mathrm{c}}. \tag{2.4}$$

The total power used in the system includes not only the transmit power of all nodes, but also the circuit power in the source, relays and destination nodes. Without loss of generality, we assume that the total power consumed in the circuits of all these nodes is p_{c}. We can assume that the value of p_{c} is constant independently of the problem variables (Masoudi *et al.*, 2018;

D'Oro *et al.*, 2018; Yu *et al.*, 2016; Wang *et al.*, 2018; Singh *et al.*, 2017; Saraiva *et al.*, 2018; Li *et al.*, 2015; Nguyen *et al.*, 2015; Sokun *et al.*, 2018; Song *et al.*, 2016).

The variables r_n^{s}, and $r_{n,q}^{\mathrm{r}}$ are defined as

$$\begin{aligned} r_n^{\mathrm{s}} &= \sum_{m\in\mathcal{M}}\sum_{k\in\mathcal{K}} y_{n,m,k}^{\mathrm{s}} \cdot r_m \quad \forall n \in \mathcal{N}, \\ r_{n,q}^{\mathrm{r}} &= \sum_{q\in\mathcal{N}}\sum_{m\in\mathcal{M}}\sum_{k\in\mathcal{K}}\sum_{j\in\mathcal{J}} y_{n,q,m,k,j}^{\mathrm{r}} \cdot r_m \quad \forall n \in \mathcal{N}. \end{aligned} \tag{2.5}$$

We present in (2.6) the total data rate, R, which effectively reaches the destination nodes through the N links due to DF forwarding mechanism.

$$R = \max \sum_{n\in\mathcal{N}} \min\left\{r_n^{\mathrm{s}}, r_{n,q}^{\mathrm{r}}\right\}. \tag{2.6}$$

Note that R can be rewritten as $\max \sum_{n\in\mathcal{N}}\sum_{m\in\mathcal{M}}\sum_{j\in\mathcal{J}} x_{n,m,j} \cdot r_m$, provided that:

$$\sum_{m\in\mathcal{M}}\sum_{j\in\mathcal{J}} x_{n,m,j} \cdot r_m \le r_n^{\mathrm{s}}, \quad \forall n \in \mathcal{N}, \tag{2.7a}$$

$$\sum_{m\in\mathcal{M}}\sum_{j\in\mathcal{J}} x_{n,m,j} \cdot r_m \le r_{n,q}^{\mathrm{r}}, \quad \forall n \in \mathcal{N}, \tag{2.7b}$$

$$\sum_{m\in\mathcal{M}}\sum_{j\in\mathcal{J}} x_{n,m,j} = 1, \quad \forall n \in \mathcal{N}, \tag{2.7c}$$

where $x_{n,m,j}$ is an auxiliary binary variable used to linearize (2.6). Using $x_{n,m,j}$ we can also easily obtain the data rate of each destination node j, R_j, as shown below:

$$R_j = \sum_{n\in\mathcal{N}}\sum_{m\in\mathcal{M}} x_{n,m,j} \cdot r_m, \quad \forall j \in \mathcal{J}. \tag{2.8}$$

The first problem formulated consists of total transmit power minimization (TPM) problem whose objective function is the minimization of (2.4) subject to QoS constraints. Therefore, the TPM problem can be formulated as

$$\min_{\substack{y_{n,m,k}^{\mathrm{s}},\, y_{n,q,m,k,j}^{\mathrm{r}} \\ x_{n,m,j}}} \quad P, \tag{2.9a}$$

$$\text{s.t. } R_j \ge \xi_j, \ \ \forall j \in \mathcal{J}, \tag{2.9b}$$

(2.2), (2.3) and (2.7),

where constraint (2.9b) consists of the QoS requirements of each destination node j in terms of its required data rate, ξ_j, i.e., (2.9b) keeps the data rates of all destination nodes of the system greater than or equal to their requirements.

According to the presented definition of EE, the QoS-constrained total EE (QEE) maximization problem can be formulated as

$$\max_{\substack{y^{\mathrm{s}}_{n,m,k},\, y^{\mathrm{r}}_{n,q,m,k,j} \\ x_{n,m,j}}} \frac{R}{P}, \tag{2.10a}$$

s.t. (2.2), (2.3), (2.7), and (2.9b).

To formulate the problem of minimum individual EE maximization we need to obtain the power consumed by each destination node, P_j. For this, it is necessary to define a new binary variable $w_{n,m,k,j}$ subject to the constraints:

$$\sum_{m\in\mathcal{M}}\sum_{k\in\mathcal{K}}\sum_{j\in\mathcal{J}} w_{n,m,k,j}\cdot r_m = \sum_{m\in\mathcal{M}}\sum_{k\in\mathcal{K}} y^{\mathrm{s}}_{n,m,k}\cdot r_m, \quad \forall n\in\mathcal{N}, \tag{2.11a}$$

$$\sum_{m\in\mathcal{M}} w_{n,m,k,j} = \sum_{q\in\mathcal{N}}\sum_{m\in\mathcal{M}} y^{\mathrm{r}}_{n,q,m,k,j}, \quad \forall n\in\mathcal{N}, \forall k\in\mathcal{K}, \forall j\in\mathcal{J}, \tag{2.11b}$$

$$\sum_{m\in\mathcal{M}}\sum_{k\in\mathcal{K}}\sum_{j\in\mathcal{J}} w_{n,m,k,j} = 1, \quad \forall n\in\mathcal{N}. \tag{2.11c}$$

In this way, the idea is basically that $w_{n,m,k,j}$ obtains n, k and j from $y^{\mathrm{r}}_{n,q,m,k,j}$ and m from $y^{\mathrm{s}}_{n,m,k}$. Thus, P_j is given as

$$P_j = \sum_{n\in\mathcal{N}}\sum_{m\in\mathcal{M}}\sum_{k\in\mathcal{K}} w_{n,m,k,j}\cdot p^{\mathrm{s}}_{n,m,k} + \sum_{n,q\in\mathcal{N}}\sum_{m\in\mathcal{M}}\sum_{k\in\mathcal{K}} y^{\mathrm{r}}_{n,q,m,k,j}\cdot p^{\mathrm{r}}_{q,m,k,j} + p^{j}_{\mathrm{c}}, \forall j\in\mathcal{J}, \tag{2.12}$$

where p^{j}_{c} is the circuit power of each destination node j, and the individual EE of destination node j, EE_j, is defined as

$$EE_j = \frac{R_j}{P_j}, \quad \forall j\in\mathcal{J}. \tag{2.13}$$

Therefore, the problem of maximizing the minimum QoS-constrained individual EE (max-min QEE) to achieve fairness in resource allocation in terms of EE among all destination nodes can be formulated as

$$\max_{\substack{y^{\mathrm{s}}_{n,m,k},\, y^{\mathrm{r}}_{n,q,m,k,j} \\ x_{n,m,j},\, w_{n,m,k,j}}} \min\left\{\frac{R_1}{P_1}, \frac{R_2}{P_2}, \ldots, \frac{R_j}{P_j}, \ldots, \frac{R_J}{P_J}\right\}, \tag{2.14}$$

s.t. (2.2), (2.3), (2.7), (2.9b) and (2.11).

Note that the objective of problem (2.14) garantees more fariness between destination nodes in terms of EE by enhancing the worst individual EE.

2.4 Simplification of Problems

The worst-case computational complexities to obtain the optimal solution for problems (2.9), (2.10) and (2.14) are exponential which certainly requires high computational performance. Fortunately, we can exploit a specific property of the DF relay mechanism to simplify all these problems in order to reduce their complexities. Firstly, we demonstrate in Proposition 1 an important property of the DF protocol applicable to problem (2.10). After that, we show how this property can be used in problems (2.9) and (2.14).

Proposition 1. *Let $\mathcal{S}$ be a set containing all possible optimal solutions of problem* (2.10)*. Then for every solution $\{y^{\mathrm{s}}_{n,m,k}, y^{\mathrm{r}}_{n,q,m,k,j}\} \in \mathcal{S}$ we necessarily have $r^{\mathrm{s}}_{n} = r^{\mathrm{r}}_{n,q}, \quad \forall n \in \mathcal{N}$.*

Demonstração. Suppose there is an optimal solution $\{y^{\mathrm{s}^\star}_{n,m,k}, y^{\mathrm{r}^\star}_{n,q,m,k,j}\} \in \mathcal{S}$ such that $r^{\mathrm{s}^\star}_{n} \neq r^{\mathrm{r}^\star}_{n,q}$ for some $n \in \mathcal{N}$, where $r^{\mathrm{s}^\star}_{n}$ is the transmit data rate in the n-th subcarrier of hop 1 associated to that solution and $r^{\mathrm{r}^\star}_{n,q}$ is the transmit data rate in the q-th subcarrier of hop 2 that is paired with the n-th subcarrier of hop 1 associated to the same solution. We can represent the data rates $r^{\mathrm{s}^\star}_{n}$ and $r^{\mathrm{r}^\star}_{n,q}$ using the link adaptation function $\varphi(\cdot)$ defined in Section 2.2. With this, we have:

$$\begin{aligned} r^{\mathrm{s}^\star}_{n} &= \varphi(\rho^{\mathrm{s}^\star}_{n} \cdot \mathrm{g}^{\mathrm{s}^\star}_{n}), \quad \forall n \in \mathcal{N}, \\ r^{\mathrm{r}^\star}_{n,q} &= \varphi(\rho^{\mathrm{r}^\star}_{n,q} \cdot \mathrm{g}^{\mathrm{r}^\star}_{n,q}), \quad \forall n \in \mathcal{N}, \end{aligned} \tag{2.15}$$

where $\rho^{\mathrm{s}^\star}_{n}$ and $\mathrm{g}^{\mathrm{s}^\star}_{n}$ are the transmit power and the normalized gain of subcarrier n in hop 1 obtained from solution $\{y^{\mathrm{s}^\star}_{n,m,k}, y^{\mathrm{r}^\star}_{n,q,m,k,j}\} \in \mathcal{S}$, respectively[3]. Analogously, $\rho^{\mathrm{r}^\star}_{n,q}$ and $\mathrm{g}^{\mathrm{r}^\star}_{n,q}$ are the transmit power and normalized gain of subcarrier q of hop 2 paired with subcarrier n in hop 1 for that particular solution, respectively. $\rho^{\mathrm{s}^\star}_{n}$, $\rho^{\mathrm{r}^\star}_{n,q}$, $\mathrm{g}^{\mathrm{s}^\star}_{n}$ and $\mathrm{g}^{\mathrm{r}^\star}_{n,q}$ are shown in (2.16a), (2.16b), (2.16c), and (2.16d), respectively.

$$\rho^{\mathrm{s}^\star}_{n} = \sum_{m\in\mathcal{M}} \sum_{k\in\mathcal{K}} y^{\mathrm{s}^\star}_{n,m,k} \cdot p^{\mathrm{s}}_{n,m,k}, \ \forall n \in \mathcal{N}, \tag{2.16a}$$

$$\rho^{\mathrm{r}^\star}_{n,q} = \sum_{q\in\mathcal{N}} \sum_{m\in\mathcal{M}} \sum_{k\in\mathcal{K}} \sum_{j\in\mathcal{J}} y^{\mathrm{r}^\star}_{n,q,m,k,j} \cdot p^{\mathrm{r}}_{q,m,k,j}, \ \forall n \in \mathcal{N}, \tag{2.16b}$$

$$\mathrm{g}^{\mathrm{s}^\star}_{n} = \sum_{m\in\mathcal{M}} \sum_{k\in\mathcal{K}} y^{\mathrm{s}^\star}_{n,m,k} \cdot \tilde{\mathrm{g}}^{\mathrm{s}}_{n,k}, \ \forall n \in \mathcal{N}, \tag{2.16c}$$

$$\mathrm{g}^{\mathrm{r}^\star}_{n,q} = \sum_{q\in\mathcal{N}} \sum_{m\in\mathcal{M}} \sum_{k\in\mathcal{K}} \sum_{j\in\mathcal{J}} y^{\mathrm{r}^\star}_{n,q,m,k,j} \cdot \tilde{\mathrm{g}}^{\mathrm{r}}_{q,k,j}, \forall n \in \mathcal{N}, \tag{2.16d}$$

where $\tilde{\mathrm{g}}^{\mathrm{s}}_{n,k} = \frac{\alpha^{\mathrm{s}}_{k} \cdot |h^{\mathrm{s}}_{n,k}|^2}{\sigma^2}$ and $\tilde{\mathrm{g}}^{\mathrm{r}}_{q,k,j} = \frac{\alpha^{\mathrm{r}}_{k,j} \cdot |h^{\mathrm{r}}_{q,k,j}|^2}{\sigma^2}$.

[3] The normalized gain is the ratio of the channel gain and the average noise power of a subcarrier.

Thus, if we have $r_n^{s^\star} \neq r_{n,q}^{r^\star}$ for some $n \in \mathcal{N}$ then we have two possibilities. Firstly, if $r_n^{s^\star} > r_{n,q}^{r^\star} \longrightarrow \rho_n^{s^\star} \cdot g_n^{s^\star} > \rho_{n,q}^{r^\star} \cdot g_{n,q}^{r^\star}$ because $\varphi(\cdot)$ is monotonically increasing. With this, we can observe that the end-to-end data rate in the link n is $r_{n,q}^{r^\star}$ [4]. Thus, it is possible to save power from link n by removing a quantity of power, $\Delta\rho_n^{s^\star}$, from subcarrier n of hop 1 so that there is no change in the end-to-end link data rate. Therefore, $0 \leq \Delta\rho_n^{s^\star} \leq \rho_n^{s^\star}$ is such that $(\rho_n^{s^\star} - \Delta\rho_n^{s^\star}) \cdot g_n^{s^\star} = \rho_{n,q}^{r^\star} \cdot g_{n,q}^{r^\star}$ when $r_n^{s^\star} = r_{n,q}^{r^\star}$. According to this hypothesis, we can decrease the used power in the system maintaining the same transmit data rate. In other words, as we assumed that the EE is defined as the ratio between the transmit data rate and the total used power, a reduction in the total used power while maintaining the same transmit data rate would lead to an improvement in the system EE. However, this is a contradiction because $\{y_{n,m,k}^{s^\star}, y_{n,q,m,k,j}^{r^\star}\}$ was a supposedly an optimal solution and its objective function, EE, could not be further increased. The same reasoning applies in the second case when $r_n^{s^\star} < r_{n,q}^{r^\star}$. Therefore, if $\{y_{n,m,k}^{s^\star}, y_{n,q,m,k,j}^{r^\star}\}$ is an optimal solution of problem (2.10), then we necessarily have $r_n^{s^\star} = r_{n,q}^{r^\star}, \quad \forall n \in \mathcal{N}$.

□

Note that an immediate consequence of Proposition 1 is that if $\{y_{n,m,k}^{s^\star}, y_{n,q,m,k,j}^{r^\star}\}$ is an optimal solution of problem (2.9) where the objective is to minimize the total transmit power, then we also necessarily have $r_n^{s^\star} = r_{n,q}^{r^\star}, \quad \forall n \in \mathcal{N}$. This is not the case for optimization objectives that involve the maximization of the spectral efficiency, e.g., total data rate maximization.

Now, for problem (2.14), suppose there is an optimal solution, $\{y_{n,m,k}^{s'}, y_{n,q,m,k,j}^{r'}\}$, where for some link there is an inequality in transmit data rates of paired subcarriers and let ε be the largest value such that:

$$\frac{R_j(\{y_{n,m,k}^{s'}, y_{n,q,m,k,j}^{r'}\})}{P_j(\{y_{n,m,k}^{s'}, y_{n,q,m,k,j}^{r'}\})} \geq \varepsilon, \ \forall j \in \mathcal{J}. \tag{2.17}$$

However, according to Proposition 1, from $\{y_{n,m,k}^{s'}, y_{n,q,m,k,j}^{r'}\}$ it is possible to find a solution, $\{y_{n,m,k}^{s^\star}, y_{n,q,m,k,j}^{r^\star}\}$, which decreases the used power in the system maintaining the same transmit data rate in order to improve EE. Thus, according to Proposition 1 in $\{y_{n,m,k}^{s^\star}, y_{n,q,m,k,j}^{r^\star}\}$, the transmit data rates of any paired subcarriers is the same but total transmit power can be lower than in solution $\{y_{n,m,k}^{s'}, y_{n,q,m,k,j}^{r'}\}$ so that:

$$\frac{R_j(\{y_{n,m,k}^{s^\star}, y_{n,q,m,k,j}^{r^\star}\})}{P_j(\{y_{n,m,k}^{s^\star}, y_{n,q,m,k,j}^{r^\star}\})} \geq \frac{R_j(\{y_{n,m,k}^{s'}, y_{n,q,m,k,j}^{r'}\})}{P_j(\{y_{n,m,k}^{s'}, y_{n,q,m,k,j}^{r'}\})} \geq \varepsilon, \ \forall j \in \mathcal{J}. \tag{2.18}$$

[4] This is a consequence of DF protocol that limits the data rate by the worst hop.

Hence, if $\{y^{s'}_{n,m,k}, y^{r'}_{n,q,m,k,j}\}$ is the optimal solution of problem (2.14) then $\{y^{s^\star}_{n,m,k}, y^{r^\star}_{n,q,m,k,j}\}$ is as well since the objective in that problem is to maximize the minimum EE among all destination nodes. Differently from problems (2.9) and (2.10), the same transmit data rates in both hops of two paired subcarriers are not necessarily required for the optimal solution of problem (2.14). However, for each optimal solution with unbalanced data rates for two paired subcarriers, there is exists an alternative optimal solution with balanced data rates for the same paired subcarriers.

Tabela 3 – Number of variables and constraints before and after applying Proposition 1.

Before applying Proposition 1		
Problems	Number of variables	Number of constraints
(2.9) and (2.10)	$NM(K+NKJ+J)$	$6N+NK+K+J+1$
(2.14)	$NM(NKJ+KJ+K+J)$	$8N+NK(J+1)+K+J+1$
After applying Proposition 1		
Problems	Number of variables	Number of constraints
(2.20), (2.21) and (2.22)	N^2MKJ	$2N+K+J+1$

The main consequence of Proposition 1 is that in the optimal solutions of problems (2.9), (2.10) and (2.14) two paired subcarriers should transmit at the same MCS level. In this way, we can define a single binary optimization variable $y_{n,q,m,k,j}$ that assumes 1 when the pair of subcarriers (n,q) matched by the k-th relay transmits at the m-th MCS level and is assigned to the j-th destination node, otherwise, we have $y_{n,q,m,k,j}=0$. Then, the link (n,q) can only transmit in a single level of MCS and only be paired by a single relay and, in addition, any subcarrier can only be paired with a single subcarrier. This allows us to rewrite the variables R, R_j, P and P_j as shown in (2.19a), (2.19b), (2.19c) and (2.19d), respectively. In summary, the main consequence of Proposition 1 is that we can rewrite problems (2.9), (2.10) and (2.14) employing a lower-dimension optimization variable, $y_{n,q,m,k,j}$, according to equations (2.20), (2.21) and (2.22), respectively.

$$R = \sum_{n,q\in\mathcal{N}} \sum_{m\in\mathcal{M}} \sum_{k\in\mathcal{K}} \sum_{j\in\mathcal{J}} y_{n,q,m,k,j} \cdot r_m, \tag{2.19a}$$

$$R_j = \sum_{n,q\in\mathcal{N}} \sum_{m\in\mathcal{M}} \sum_{k\in\mathcal{K}} y_{n,q,m,k,j} \cdot r_m, \quad \forall j \in \mathcal{J}, \tag{2.19b}$$

$$P = \sum_{n,q\in\mathcal{N}} \sum_{m\in\mathcal{M}} \sum_{k\in\mathcal{K}} \sum_{j\in\mathcal{J}} y_{n,q,m,k,j} \cdot (p^{\mathrm{s}}_{n,m,k} + p^{\mathrm{r}}_{q,m,k,j}) + p_{\mathrm{c}}, \tag{2.19c}$$

$$P_j = \sum_{n,q\in\mathcal{N}} \sum_{m\in\mathcal{M}} \sum_{k\in\mathcal{K}} y_{n,q,m,k,j} \cdot (p^{\mathrm{s}}_{n,m,k} + p^{\mathrm{r}}_{q,m,k,j}) + p^{j}_{\mathrm{c}}, \quad \forall j \in \mathcal{J}. \tag{2.19d}$$

$$\min_{y_{n,q,m,k,j}} P, \tag{2.20a}$$

$$\text{s.t.} \sum_{n,q\in\mathcal{N}} \sum_{m\in\mathcal{M}} \sum_{k\in\mathcal{K}} y_{n,q,m,k,j} \cdot r_m \geq \xi_j, \quad \forall j \in \mathcal{J}, \tag{2.20b}$$

$$\sum_{n\in\mathcal{N}} \sum_{m\in\mathcal{M}} \sum_{k\in\mathcal{K}} \sum_{j\in\mathcal{J}} y_{n,q,m,k,j} = 1, \quad \forall q \in \mathcal{N}, \tag{2.20c}$$

$$\sum_{q\in\mathcal{N}} \sum_{m\in\mathcal{M}} \sum_{k\in\mathcal{K}} \sum_{j\in\mathcal{J}} y_{n,q,m,k,j} = 1, \quad \forall n \in \mathcal{N}, \tag{2.20d}$$

$$\sum_{n,q\in\mathcal{N}} \sum_{m\in\mathcal{M}} \sum_{k\in\mathcal{K}} \sum_{j\in\mathcal{J}} y_{n,q,m,k,j} \cdot p^{\mathrm{s}}_{n,m,k} \leq P^{\mathrm{s}}_{\text{total}}, \tag{2.20e}$$

$$\sum_{n,q\in\mathcal{N}} \sum_{m\in\mathcal{M}} \sum_{j\in\mathcal{J}} y_{n,q,m,k,j} \cdot p^{\mathrm{r}}_{q,m,k,j} \leq P^{k}_{\text{total}}, \quad \forall k \in \mathcal{K}, \tag{2.20f}$$

$$\max_{y_{n,q,m,k,j}} \frac{R}{P}, \tag{2.21a}$$

s.t. (2.20b), (2.20c), (2.20d), (2.20e) and (2.20f).

and problem (2.14) as:

$$\max_{y_{n,q,m,k,j}} \min \left\{ \frac{R_1}{P_1}, \frac{R_2}{P_2}, \ldots, \frac{R_j}{P_j}, \ldots, \frac{R_J}{P_J} \right\}, \tag{2.22a}$$

s.t. (2.20b), (2.20c), (2.20d), (2.20e) and (2.20f).

We show in Table 3 the number of binary optimization variables and constraints for problems (2.9), (2.10), and (2.14) before and after applying Proposition 1, which leads to a significant simplification of the problems formulated in Section 2.3.

2.5 Optimal Solutions

In this section, we discuss the optimal solutions to the problems (2.20), (2.21) and (2.22). Before this, firstly, note that linear constraints (2.20b), (2.20c), (2.20d), (2.20e) and (2.20f) are common to all three problems and we can represent them in matrix form, respectively, as follows:

$$\left[\mathbf{1}_{1\times N^2} \otimes \left[\mathbf{r}^T \otimes \left[\mathbf{1}_{1\times K} \otimes \mathbf{I}_J\right]\right]\right] \mathbf{y} \geq \boldsymbol{\xi}, \tag{2.23a}$$

$$\left[\mathbf{1}_{1\times N} \otimes \left[\mathbf{I}_N \otimes \mathbf{1}_{1\times MKJ}\right]\right] \mathbf{y} = \mathbf{1}_{N\times 1}, \tag{2.23b}$$

$$\left[\mathbf{I}_N \otimes \mathbf{1}_{1\times NMKJ}\right] \mathbf{y} = \mathbf{1}_{N\times 1}, \tag{2.23c}$$

$$\left[\mathbf{1}_{1\times N} \otimes \left[\left[\mathbf{p}_1^{\mathrm{s}}\right]^T \otimes \mathbf{1}_{1\times J}\right], \ldots, \mathbf{1}_{1\times N} \otimes \left[\left[\mathbf{p}_N^{\mathrm{s}}\right]^T \otimes \mathbf{1}_{1\times J}\right]\right] \mathbf{y} \leq \mathbf{p}_{\text{total}}^{\mathrm{s}}, \tag{2.23d}$$

$$\left[\mathbf{1}_{1\times N} \otimes \left[\left[\mathbf{1}_{1\times NM} \otimes \left[\mathbf{I}_K \otimes \mathbf{1}_{1\times J}\right]\right] \odot \left[\mathbf{1}_{K\times 1} \otimes \left[\mathbf{p}^{\mathrm{r}}\right]^T\right]\right]\right] \mathbf{y} \leq \mathbf{p}_{\text{total}}^{\mathrm{r}}, \tag{2.23e}$$

where $\mathbf{1}_{v\times u}$ is a $v \times u$ matrix composed by 1's, $\mathbf{I}_a$ is an $a \times a$ identity matrix and the operators $\otimes$, $\odot$ and $(\cdot)^T$ are the Kronecker product, the Hadamard product and the transpose matrix, respectively. Furthermore, we assume $\mathbf{r} = [r_1, \ldots, r_M]^T$, $\boldsymbol{\xi} = [\xi_1, \ldots, \xi_J]^T$, $\mathbf{p}_n^{\mathrm{s}} = [p_{n,1,1}^{\mathrm{s}}, \ldots, p_{n,M,K}^{\mathrm{s}}]^T$, $\forall n \in \mathcal{N}$, $\mathbf{p}_{\text{total}}^{\mathrm{s}} = [P^{\mathrm{s}}]$, $\mathbf{p}_{\text{total}}^{\mathrm{r}} = [P^1, \ldots, P^K]^T$ and, finally, $\mathbf{y} = [y_{1,1,1,1,1}, y_{1,1,1,1,2}, \ldots, y_{N,N,M,K,J}]^T$, which is the vector of optimization variables.

Based on the knowledge of the problem constraints in equations (2.23), we can define the set $\boldsymbol{\Upsilon}$ as as the solution space of optimization problems (2.20), (2.21) and (2.22). $\boldsymbol{\Upsilon}$ is defined in (2.24) where $\mathcal{B}$ is a set of binary vectors such that $z = N^2MKJ$.

$$\boldsymbol{\Upsilon} = \left\{\mathbf{y} \mid \mathbf{A}\mathbf{y} \leq \mathbf{b}, \boldsymbol{\Lambda}\mathbf{y} = \mathbf{d},\ \mathbf{y} \in \mathcal{B}^{z\times 1}\right\}, \tag{2.24a}$$

$$\mathbf{A} = \begin{bmatrix} \mathbf{1}_{1\times N^2} \otimes \left[\mathbf{r}^T \otimes \left[\mathbf{1}_{1\times K} \otimes \mathbf{I}_J\right]\right] \\ \mathbf{1}_{1\times N} \otimes \left[\left[\mathbf{p}_1^{\mathrm{s}}\right]^T \otimes \mathbf{1}_{1\times J}\right], \ldots, \mathbf{1}_{1\times N} \otimes \left[\left[\mathbf{p}_N^{\mathrm{s}}\right]^T \otimes \mathbf{1}_{1\times J}\right] \\ \mathbf{1}_{1\times N} \otimes \left[\left[\mathbf{1}_{1\times NM} \otimes \left[\mathbf{I}_K \otimes \mathbf{1}_{1\times J}\right]\right] \odot \left[\mathbf{1}_{K\times 1} \otimes \left[\mathbf{p}^{\mathrm{r}}\right]^T\right]\right] \end{bmatrix}, \mathbf{b} = \begin{bmatrix} -\boldsymbol{\xi} \\ \mathbf{p}_{\text{total}}^{\mathrm{s}} \\ \mathbf{p}_{\text{total}}^{\mathrm{r}} \end{bmatrix},$$

$$\boldsymbol{\Lambda} = \begin{bmatrix} \mathbf{1}_{1\times N} \otimes \left[\mathbf{I}_N \otimes \mathbf{1}_{1\times MKJ}\right] \\ \mathbf{I}_N \otimes \mathbf{1}_{1\times NMKJ} \end{bmatrix} \text{ and } \mathbf{d} = \begin{bmatrix} \mathbf{1}_{N\times 1} \\ \mathbf{1}_{N\times 1} \end{bmatrix},$$

Moreover, we can also represent the variables R, R_j, P and P_j in matrix form as shown in (2.25a), (2.25b), (2.25c) and (2.25d), respectively. $\boldsymbol{\theta}_j$ and $\boldsymbol{\vartheta}_j$ are the j-th rows of

matrices $\mathbf{R}_{\mathrm{j}}$ and $\mathbf{P}_{\mathrm{j}}$ defined in (2.26), respectively [5].

$$R = \left[\mathbf{1}_{1\times N^2} \otimes \left[\mathbf{r}^T \otimes [\mathbf{1}_{1\times KJ}]\right]\right] \mathbf{y}, \tag{2.25a}$$

$$R_j = \boldsymbol{\theta}_j \mathbf{y}, \tag{2.25b}$$

$$P = \left[[\mathbf{p}^{\mathrm{s}*}]^T + \mathbf{1}_{1\times N} \otimes [\mathbf{p}^{\mathrm{r}}]^T\right] \mathbf{y} + p_{\mathrm{c}}, \tag{2.25c}$$

$$P_j = \boldsymbol{\vartheta}_j \mathbf{y} + p_{\mathrm{c}}^j. \tag{2.25d}$$

$$\mathbf{R}_{\mathrm{j}} = \left[\mathbf{1}_{1\times N^2} \otimes \left[\mathbf{r}^T \otimes [\mathbf{1}_{1\times K} \otimes \mathbf{I}_J]\right]\right], \tag{2.26a}$$

$$\mathbf{P}_{\mathrm{j}} = \left[[\mathbf{P}^{\mathrm{s}*}] + \mathbf{1}_{1\times N} \otimes \left[[\mathbf{1}_{1\times NMK} \otimes \mathbf{I}_J] \odot [\mathbf{1}_{J\times 1} \otimes [\mathbf{p}^{\mathrm{r}}]^T]\right]\right], \tag{2.26b}$$

where

$$\mathbf{P}^{\mathrm{s}*} = \left[\mathbf{1}_{1\times N} \otimes \left[[\mathbf{p}_1^{\mathrm{s}}]^T \otimes \mathbf{I}_J\right], \ldots, \mathbf{1}_{1\times N} \otimes \left[[\mathbf{p}_N^{\mathrm{s}}]^T \otimes \mathbf{I}_J\right]\right], \tag{2.27a}$$

$$\mathbf{p}^{\mathrm{r}} = [p^r_{1,1,1,1}, p^r_{1,1,1,2}, \ldots, p^r_{N,M,K,J}]^T. \tag{2.27b}$$

Therefore, we can finally rewrite the problems (2.20), (2.21) and (2.22) in their final forms as presented in (2.28a), (2.28b) and (2.28c), respectively.

$$\min_{\mathbf{y}\in\boldsymbol{\Upsilon}} P(\mathbf{y}), \tag{2.28a}$$

$$\max_{\mathbf{y}\in\boldsymbol{\Upsilon}} \frac{R(\mathbf{y})}{P(\mathbf{y})}, \tag{2.28b}$$

$$\max_{\mathbf{y}\in\boldsymbol{\Upsilon}} \min\left\{\frac{R_1(\mathbf{y})}{P_1(\mathbf{y})}, \frac{R_2(\mathbf{y})}{P_2(\mathbf{y})}, \ldots, \frac{R_j(\mathbf{y})}{P_j(\mathbf{y})}, \ldots, \frac{R_J(\mathbf{y})}{P_J(\mathbf{y})}\right\}. \tag{2.28c}$$

According to the analysis above, note that problem (2.28a) belongs to the class of integer linear problems (ILPs) and, therefore, it can be optimally solved by standard algorithms based on branch and bound (BB) method (Lawler; Wood, 1966). In general, in these algorithms for an arbitrary number of integer variables, l, the number of linear programming subproblems to be solved is at least $(\sqrt{2})^l$. Meanwhile, the number of iterations needed to solve one linear programming problem with t constraints and l variables is approximately $2(l+t)$, and each iteration encompasses $lt - t$ multiplications, $lt - t$ summations, and $l - t$ comparisons. Thus,

[5] A generic matrix expression of type $\mathbf{a}^T\mathbf{v} + s$, where s is a scalar and $\mathbf{v}$ is a vector can be rewritten equivalently as $\mathbf{a}^T\mathbf{v}$ simply making $\mathbf{a} = [\mathbf{a}^T s]^T$ and $\mathbf{v} = [\mathbf{v}^T 1]^T$.

Algoritmo 1: Dinkelbach algorithm applied in problem (2.28b)

Require: $\epsilon > 0$; $i \leftarrow 0$; $\eta_i \geq 0$;

1: $\mathbf{y}_i^\star \leftarrow \arg\max_{\mathbf{y}\in\boldsymbol{\Upsilon}} \{R(\mathbf{y}) - \eta_i \cdot P(\mathbf{y})\}$;
2: **while** $R(\mathbf{y}_i^\star) - \eta_i \cdot P(\mathbf{y}_i^\star) > \epsilon$ **do**
3: $\quad \eta_{i+1} \leftarrow \frac{R(\mathbf{y}_i^\star)}{P(\mathbf{y}_i^\star)}$;
4: $\quad \mathbf{y}_{i+1}^\star \leftarrow \arg\max_{\mathbf{y}\in\boldsymbol{\Upsilon}} \{R(\mathbf{y}) - \eta_{i+1} \cdot P(\mathbf{y})\}$; $i \leftarrow i + 1$;
5: **end while**; **return** $\mathbf{y}_{i-1}^\star$;

the required total number of operations is $\sqrt{2}^l 2(l+t)(2lt-3t+l)$ (Lima *et al.*, 2016). Based on that and according to Table 3 the worst-case computational complexity to obtain the optimal solution to problem (2.28a), retaining the term of higher order, is $\mathcal{O}(2^{N^2MKJ})$.

Unlike problem (2.28a), problems (2.28b) and (2.28c) are non-linear and their optimal solutions are usually harder to get. More specifically, problem (2.28b) is a classic problem of fractional programming with linear terms in the numerator and denominator, whose purpose is to maximize a single fractional function. The optimal solution of problem (2.28b) can be obtained by the Dinkelbach algorithm (Dinkelbach, 1967) (Algorithm 1), whose fundamental idea is to determine the root of the function in an equivalent parametric problem. This algorithm is based on a theorem by Jagannathan (Jagannathan, 1966) concerning the relationship between fractional and parametric programming as stated in Proposition 2.

Proposition 2. (Dinkelbach, 1967; Jagannathan, 1966). $\eta^\star = \frac{R(\mathbf{y}^\star)}{P(\mathbf{y}^\star)} = \max_{\mathbf{y}\in\boldsymbol{\Upsilon}} \left\{\frac{R(\mathbf{y})}{P(\mathbf{y})}\right\}$, *where* $\mathbf{y}^\star \in \boldsymbol{\Upsilon}$ *solves* (2.28b) *if and only if*

$$\max_{\mathbf{y}\in\boldsymbol{\Upsilon}} \{R(\mathbf{y}) - \eta^\star \cdot P(\mathbf{y})\} = 0. \tag{2.29}$$

In Algorithm 1 we initialize the variable η_i that is used to recast problem (2.28b) from a fractional to a subtractive form. The new subproblem, which is in a subtractive form (line 1 of Algorithm 1) belongs to the class of ILP problems. Between lines 2 and 5, the following tasks are executed iteratively: the value of η_i is redefined according to the solution obtained in line 1, a new ILP is solved and a stop criterion is evaluated. For integer or combinatorial optimization problems according to (Anzai, 1974), the convergence to the optimal solution is guaranteed if the search space is limited. Given that $\boldsymbol{\Upsilon}$ is limited due to the power and QoS constraints, the convergence of our proposed optimal solution to the problem (2.28b) is guaranteed. Thus, the Dinkelbach algorithm is able to solve integer fractional problems by solving a sequence of ILP subproblems.

Algoritmo 2: Generalized Dinkelbach algorithm applied in problem (2.28c)

Require: $\epsilon > 0$; $i \leftarrow 0$; $\eta_i \geq 0$;
1: **while** $F(\eta_i) > \epsilon$ **do**
2: $\quad \mathbf{y}_i^\star \leftarrow \arg\max_{\mathbf{y}\in\boldsymbol{\Upsilon}} \{\min_{j\in\mathcal{J}}\{R_j(\mathbf{y}) - \eta_i P_j(\mathbf{y})\}\}$;
3: $\quad F(\eta_{i+1}) \leftarrow \min_{j\in\mathcal{J}}\{R_j(\mathbf{y}_i^\star) - \eta_i P_j(\mathbf{y}_i^\star)\}$;
4: $\quad \eta_{i+1} \leftarrow \min_{j\in\mathcal{J}} \left\{\frac{R_j(\mathbf{y}_i^\star)}{P_j(\mathbf{y}_i^\star)}\right\}; i \leftarrow i+1$;
5: **end while**; **return** $\mathbf{y}_{i-1}^\star$;

When problem (2.28b) is concerned, we can note that it is less complex than problem (2.28c) since in the latter we are interested in maximizing the minimum of a set of ratios instead of only one. Indeed, problem (2.28c) can be cast into the framework of generalized fractional programming and it is formally specified as a nonlinear program where a nonlinear function defined as the minimum over several ratios of functions should be maximized. Fortunately, Dinkelbach's approach to classical fractional problems can be generalized and, consequently, the result of Proposition 2 as well. As a result, a similar approach can be applied to a generalized fractional programming problem and we formally present this result in Proposition 3.

Proposition 3. (Zappone *et al.*, 2016; Jagannathan, 1966; Crouzeix; Ferland, 1991). *A vector* $\mathbf{y}^\star \in \boldsymbol{\Upsilon}$ *solves* (2.28c) *if and only if*

$$\mathbf{y}^\star = \arg\max_{\mathbf{y}\in\boldsymbol{\Upsilon}} \left\{\min_{j\in\mathcal{J}}\{R_j(\mathbf{y}) - \eta^\star P_j(\mathbf{y})\}\right\} \tag{2.30}$$

with $\eta^\star$ *being the unique zero of the auxiliary function* $F(\eta)$:

$$F(\eta) = \max_{\mathbf{y}\in\boldsymbol{\Upsilon}} \left\{\min_{j\in\mathcal{J}}\{R_j(\mathbf{y}) - \eta P_j(\mathbf{y})\}\right\}. \tag{2.31}$$

Hence, according to Proposition 3, solving (2.28c) is equivalent to finding the unique zero of function $F(\eta)$ and its proof can be found in (Crouzeix; Ferland, 1991). As already mentioned, this result can be seen as a generalization of the approach proposed by Dinkelbach. Based on Proposition 3 the Algorithm 2 called generalized Dinkelbach algorithm can be employed to find the optimal solution to problem (2.28c). In this algorithm, it can be shown that the update rule for η follows Newton's method applied to the function $F(\eta)$. In this way, the value of η is updated at each iteration where η_0 is its initial value. According to (Zappone *et al.*, 2016), η converges to the global optimum of problem (2.28c) provided that problem (2.30) (line 2 of Algorithm 2) can be globally solved at each iteration. Given that problem (2.30) is an ILP, its optimal solution can be obtained by standard algorithms and, similarly to Algorithm 1,

Algorithm 2 solves problem (2.28c) by solving a sequence of ILP subproblems until $F(\eta) \leq \epsilon$ (line 1).

In short, the algorithms 1 and 2 solve the problems (2.28b) and (2.28c), respectively, by iteratively solving multiple instances of ILPs subproblems. Since each ILP subproblem has the same number of constraints and variables of problem (2.28a), then both Algorithm 1 and Algorithms 2 has a worst-case computational complexity $\mathcal{O}(2^{N^2MKJ})$.

2.6 Simulation Results

In this section, we evaluate the performance of the involved solutions by means of computer simulations. Firstly, we present the simulations modeling and parameters in Subsection 2.6.1 and then we discuss the obtained results.

2.6.1 Parameters and Simulation Characteristics

Tabela 4 – Simulation parameters.

Parameter	Value
Number of subcarrier	$12 - 32$
Number of relays	$1 - 5$
Number of destination nodes	4
Number of MCSs	11
Static circuit power	100 mW
Noise power spectral density	-174 dBm/Hz

We assume that the total power available in each relay is equal to the total power available at the source that is 27 dBm (Tao *et al.*, 2012). The relays are uniformly distributed over a square with area of 0.25 km^2 according to Figure 3 and similar to the scenario addressed in (Dang *et al.*, 2010).

In this work, we assume that the possible data rate transmission rates in kbps are $r_m \in \{0,\, 20,\, 40, \cdots, 200\}$, $\forall m \in \mathcal{M}$. The SNR intervals for transmission of each MCS were extracted through the discretization of the Shannon curve with $\gamma_m = 2^{r_m/B} - 1$ where $B = 15$ kHz is the band occupied by a subcarrier. The propagation effects modeled in this paper are mean path loss (Sun *et al.*, 2011), log-normal shadowing (standard deviation equal to 8 dB) (Chen *et al.*, 2017), and fast fading following a Rayleigh distribution. In addition, we assume that a central node (where resource allocation decisions are made) has perfect CSI.

Figura 3 – Scenario used in computational simulations for the problems (2.20), (2.21) and (2.22).

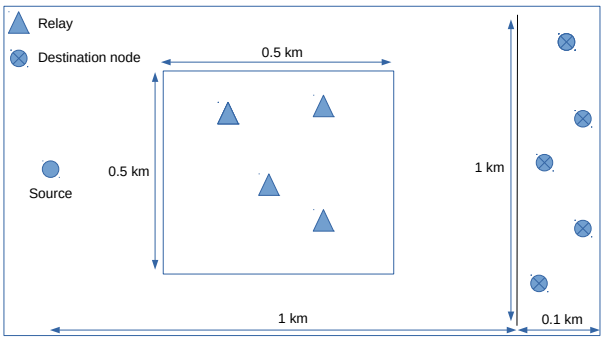

Fonte: Created by the author.

2.6.2 Discussion

In Figure 4, we have the total system EE versus the number of iterations of Algorithm 1 to solve QEE problem for different number of relays in the considered scenario. In this figure, we can observe the efficiency of Algorithm 1 since the convergence to the optimal solution is reached within few iterations. In addition, this figure also shows the gains in EE due to the additional space diversity achieved by the combination of an increased number of relays nodes and opportunistic relay selection.

In Figure 5 the total EE for the QEE and TPM problems versus the level of QoS required by the destination nodes are ploted. Firstly, we observe that the EE of QEE solution decreases with the QoS requirements. Basically, the more stringent the QoS requirement of destination nodes becomes, the harder it is to find efficient subcarrier pairing, assignment and relay selection to improve EE. On the other hand, the solution to TPM does not intend to maximize EE but to minimize the total transmit power subject to minimum QoS constraints. Therefore, the destination nodes receives only its minimum required data rate even if additional data rate would be beneficial for EE. Therefore, the EE of TPM solution achieves the maximum EE in an intermediary QoS level.

An important aspect that can be seen from Figure 5 is the convergence of the EE for QEE and TPM solutions at high QoS requirements. The reason for that behavior is straighforward: as QoS demands are increased, the number of feasible solutions (that complies with problem constraints) to both optimization problems (QEE and TPM) is considerably reduced. Thus, at high QoS requirements the QEE solution cannot deliver data rates beyond the required QoS so that the total EE is maximized by minimizing the total transmit power and this is exactly what

Figura 4 – Total energy efficiency versus the the number of iterations of Algorithm 1.

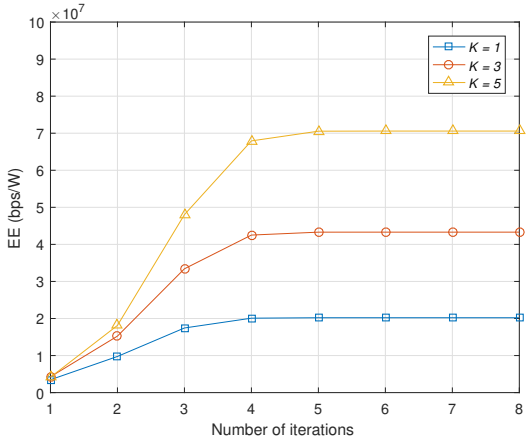

Fonte: Created by the author.

Figura 5 – Total energy efficiency versus the data rate required by destination nodes.

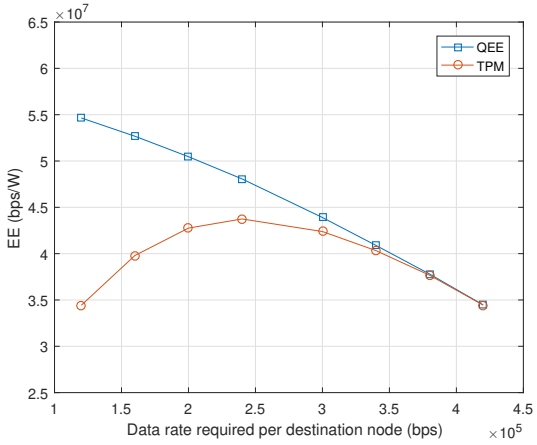

Fonte: Created by the author.

the TPM solution does. Therefore, the optimization objective function plays a less important role in this context (at high QoS demands) and the solutions to both problems tend to become similar.

From an application point of view, this result has important consequences. Basically, it shows that optimizing the EE by QEE solution is advantageous for low and medium QoS requirements. When the QoS demand is high, the solution to the TPM problem, which can be obtained by solving only one instance of an ILP problem, is similar in terms of total EE to the solution of QEE problem, which is obtained by solving an ILP problem per iteration according to Algorithm 1. This shows that the optimization of EE can be achieved with lower complexity in some scenarios.

However, when the total EE is maximized in a scenario with many destination nodes, individual EE fairness in resource allocation of all these nodes is not guaranteed. In order to maximize the total EE, it is natural to allocate most of the resources to the links in better channel conditions that can make better use of the transmit power. With this, the individual EE of each destination node in general can be quite distinct from each other which can lead to severe unfairness among them. As discussed before, the max-min QEE problem is essentially a fairness problem since its optimal solution can deliver the higher individual EE floor as shown in Figure 6, which shows the CDFs for the minimum individual EE of the QEE, TPM and max-min QEE problems. Roughly speaking, max-min QEE solution is the one that most cares about the worst destination node and the impact of this is a high fairness among the individual EE of all destination nodes of the system. Indeed, this can be viewed in Figure 7, which shows

Figura 6 – CDF for the minimum individual energy efficiency of the QEE, TPM and max-min QEE problems.

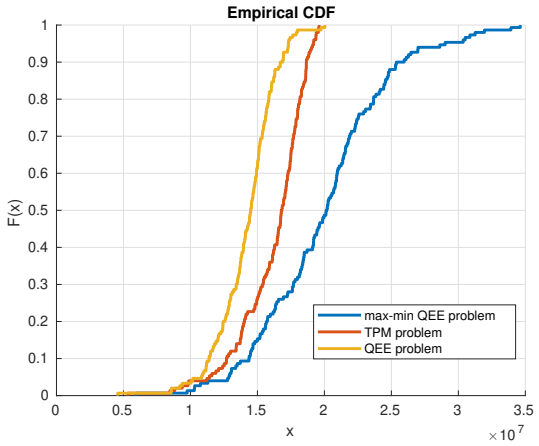

Fonte: Created by the author.

Figura 7 – Individual energy efficiency versus the number of iterations of Algorithm 2.

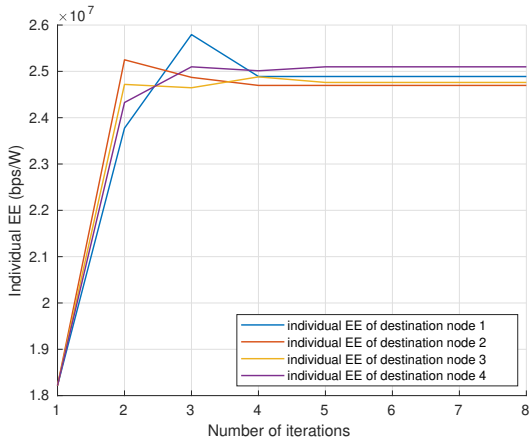

Fonte: Created by the author.

the individual EE versus the number of iterations of Algorithm 2. Note in this figure that the individual EE converges to very close values, proving that the max-min QEE solution can ensure fairness among all destination nodes in terms of EE.

However, although Figure 7 shows the convergence of the individual EE to very close values, it does not show numerically the fairness level achieved. One well known way to quantitatively measure the fairness level is to employ the Jain's fairness index (Jain *et al.*, 1984). It is defined as a continuous non-convex function $I(\cdot)$ such that for the EEs shown in (2.13) we have $I(EE_1, \ldots, EE_J) = \frac{\left(\sum_{\forall j \in \mathcal{J}} EE_j\right)^2}{J \sum_{\forall j \in \mathcal{J}} EE_j^2}$ with values in the interval $[\frac{1}{J}, 1]$, i.e., it ranges from $\frac{1}{J}$ to 1 so that a large value of $I(\cdot)$ represents fairer resource allocation from the system perspective (Huaizhou *et al.*, 2014).

Taking this into account, in Figure 8 we plot $I(EE_1, \ldots, EE_J)$ for the three problems addressed in this chapter versus the level of QoS required by the destination nodes. Note firstly that $I(EE_1, \ldots, EE_J)$ for the max-min QEE problem is practically constant and very close to 1 (maximum value of $I(EE_1, \ldots, EE_J)$) independent of QoS requirements. This is an expected result according to Figure 6 and Figure 7. In Figure 8 we highlight $I(EE_1, \ldots, EE_J)$ for QEE problem that grows with the increase of QoS requirements, i.e., the resource allocation of QEE problem becomes fairer in terms of EE as more data rate is required by destination nodes. This shows that very unfair resource allocation in terms of EE tends to occur only at low QoS requirements and the reason for this is very simple: only at low QoS requirements is it possible to assign more resources to the destination nodes in better channel conditions to

Figura 8 – Jain's fairness index (Jain *et al.*, 1984) versus the data rate required by destination nodes.

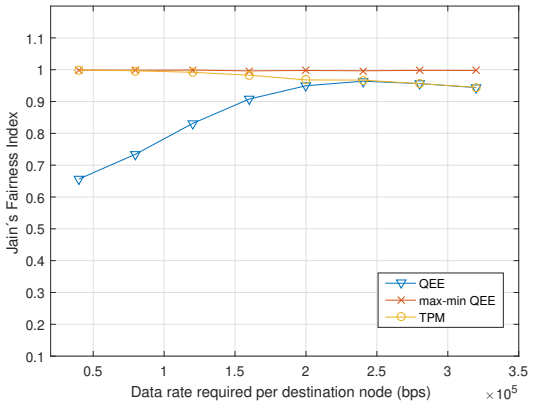

Fonte: Created by the author.

Figura 9 – Total energy efficiency versus the data rate required by destination nodes.

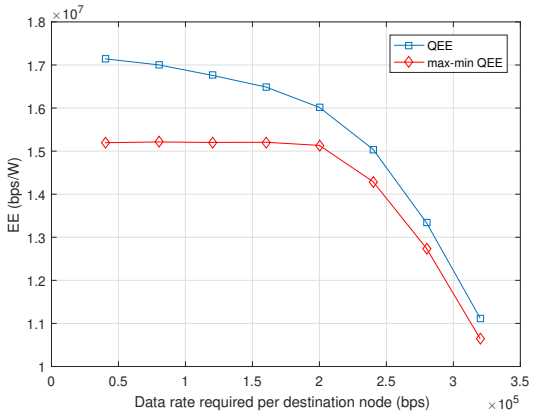

Fonte: Created by the author.

improve EE. As QoS demands are increased, the trend is that QoS is only minimally satisfied for all the destination nodes so that the individual EE are naturally similar. This result is particularly interesting because it shows that at high QoS requirements, besides being possible to obtain the maximization of total EE more easily by using TPM solution as shown previously, fairness in resource allocation in terms of EE among all destination nodes is also guaranteed.

Finally, we show in Figure 9 the total EE for the QEE and max-min QEE problems versus the level of QoS required by the destination nodes. In this figure, note first that offering fairness in resource allocation can result in considerable losses to the total EE. However, the greatest losses only tend to occur at low QoS requirements, since for high requirements the total EE for the QEE and max-min QEE problems become closer. In fact, this behavior is expected due to the result of Figure 8.

2.7 Partial Conclusions

In this chapter we studied the problems of total EE maximization, total power minimization and minimum individual EE maximization in a cooperative scenario with multiple relays and destination nodes assuming QoS constraints. The problems of total EE maximization and minimum individual EE maximization were formulated as fractional integer optimization problems. By using fractional and generalized fractional programming theory, we were able to obtain the optimal solution to these problems by solving a sequence of integer linear subproblems.

By identifying an important property through the analysis of the signal processing done in the relays, we were able to considerably reduce the size of the three optimization problems. Finally, we compared the performance of the total EE for the three problems discussed in this paper and also discussed about fairness in resource allocation among all destination nodes. One important conclusion obtained from the results was that at high QoS requirements the total EE is maximized even when the problem objective is to minimize the total transmit power. Therefore, the EE maximization can be obtained with simpler algorithms when the QoS demand is high.

3 FAIRNESS-ORIENTED POWER ALLOCATION IN ENERGY HARVESTING AIDED MASSIVE MIMO SYSTEMS

3.1 Introduction

In this chapter, we consider an EH-aided massive MIMO system and investigate the fairness problem of maximizing the minimum system SINR while fulfilling QoS requirements. This chapter is organized as follows. Section 3.2 provides the system modeling and EH model. The mathematical formulation of the problem discussed in this chapter is presented in Section 3.3. In Section 3.4 we provide the optimal solution of the formulated problem and we present an alternative solution for it. Section 3.5 presents numerical results to evaluate the performance of these proposals and other discussions. Finally, Section 3.6 concludes the chapter by summarizing and highlighting its main points.

3.2 Channel and Signal Modeling

The studied system consists of a coverage area with N H-APs that simultaneously serve in the downlink K terminals[1] in the same time-frequency resource with $N \gg K$. All H-APs and terminals are equipped with a single antenna and they are randomly located in a large area. We consider that each H-AP is powered by the electrical grid and additionally owns a battery that is connected to an EH source. Furthermore, all H-APs are connected to a central processing unit via fast backhaul links, which allows important information exchanges such as battery levels, pilot signals, precoders information, etc. The set of H-APs and terminals comprises a distributed massive MIMO system illustrated in Figure 10. We assume that the central processing unit has perfect CSI. We consider the transmission process along L successive time transmission time intervals (TTIs) with duration equal to τ. According to the previous definitions we can define the following sets: $\mathcal{N} = \{1, \ldots, N\}$ as the set of all H-APs, $\mathcal{K} = \{1, \ldots, K\}$ the set of all terminals and $\mathcal{L} = \{1, \ldots, L\}$ the set of all TTIs. The channel coefficients between the H-APs and the terminals are represented by a complex matrix $\mathbf{G}^l = [\mathbf{g}_1^l, \mathbf{g}_2^l, \ldots, \mathbf{g}_K^l]$ in which $\mathbf{g}_k^l = [\mathrm{g}_{n,k}^l]_{n \in \mathcal{N}} \in \mathbb{C}^{N \times 1}$ is the column channel vector of terminal $k \in \mathcal{K}$ at TTI $l \in \mathcal{L}$. As we assume non co-located transmit and receive antennas, the spatial correlation is neglected. The channel coefficient $\mathrm{g}_{n,k}^l$ is given by $\mathrm{g}_{n,k}^l = \sqrt{\beta_{n,k}} h_{n,k}^l$, where $h_{n,k}^l$ is the small-scale component fading at TTI $l \in \mathcal{L}$ for H-AP $n \in \mathcal{N}$ and user $k \in \mathcal{K}$ and $\beta_{n,k}$ represents the large-scale fading

[1] In this chapter, we assume that each user owns a mobile terminal and is engaged in a data session. Therefore, the terms "user" and "terminal" are interchangeable in the chapter.

Figura 10 – Distributed massive MIMO system in which each H-AP is powered by both an independent EH source and the electrical grid.

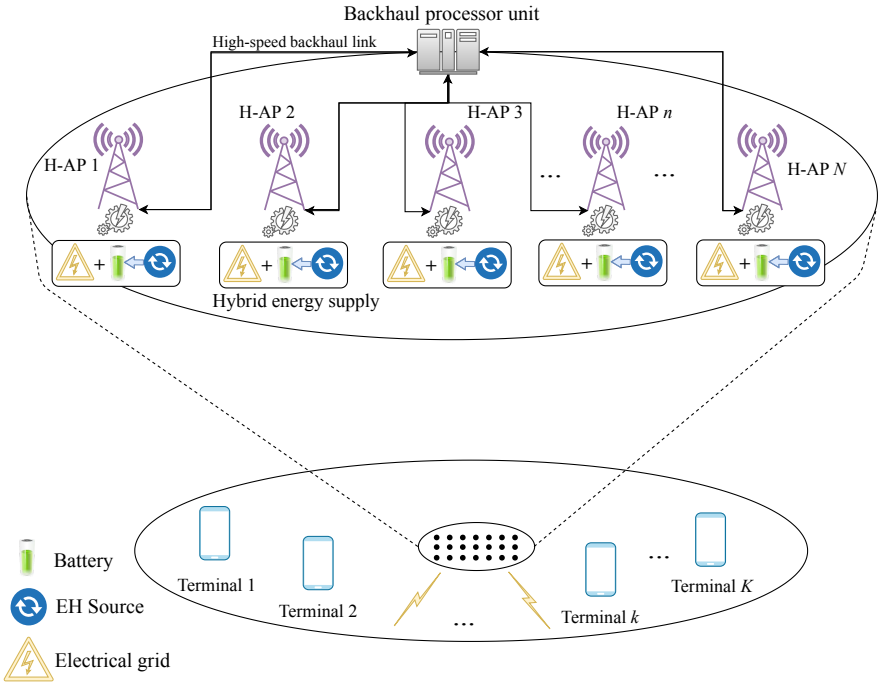

Fonte: Created by the author.

component between user $k \in \mathcal{K}$ and H-AP $n \in \mathcal{N}$. The small-scale fading $h^l_{n,k}$ is assumed to be quasi-static Gaussian independent and identically distributed (i.i.d.). The large-scale fading component is expressed as $\beta_{n,k} = \zeta \frac{d^{-\nu}_{n,k}}{d^{-\nu}_{\text{o}}}$, where ν is the path loss exponent, $d_{n,k}$ is the distance between H-AP $n \in \mathcal{N}$ and terminal $k \in \mathcal{K}$, d_{o} is the reference distance and ζ is a constant related to the carrier frequency and reference distance.

We denote by $\mathbf{w}^l_k \in \mathbb{C}^{1\times N}$ the k-th beamforming vector for terminal $k \in \mathcal{K}$ at TTI $l \in \mathcal{L}$. The low complexity maximum ratio transmission (MRT) is considered as beamforming technique. The beamforming vector for terminal $k \in \mathcal{K}$ and TTI $l \in \mathcal{L}$ is given by $\mathbf{w}^l_k = \frac{(\mathbf{g}^l_k)^H}{||(\mathbf{G}^l)^H||_{\text{F}}}$, where $||\cdot||_{\text{F}}$ denotes the Frobenius norm of a matrix and $(\cdot)^H$ represents the conjugate transpose or Hermitian transpose of a matrix. Hence, the received SINR at terminal $k \in \mathcal{K}$ and at TTI $l \in \mathcal{L}$ is expressed as:

$$\gamma_{k,l} = \frac{\sum_{n\in\mathcal{N}} \rho_{n,k,l} \mid \mathbf{w}^l_k \mathbf{g}^l_k \mid^2}{\sum_{\tilde{k}\in\mathcal{K},\tilde{k}\neq k} \sum_{n\in\mathcal{N}} \rho_{n,\tilde{k},l} \mid \mathbf{w}^l_{\tilde{k}} \mathbf{g}^l_k \mid^2 + \sigma^2}, \tag{3.1}$$

where $\rho_{n,k,l}$ is the transmit power allocated to terminal $k \in \mathcal{K}$ on H-AP $n \in \mathcal{N}$ at TTI $l \in \mathcal{L}$ and σ^2 is the variance of the noise that is assumed to be additive white Gaussian noise (AWGN) with zero mean.

3.2.1 Energy Harvesting Model

The harvested energy at each H-AP is first stored in a battery with limited storage capabilities that can store at most $B_{\max}$ units of energy. On the matter of harvest dynamics, we consider a first-order stationary Markov model for solar radiation similar to addressed in (Carvalho *et al.*, 2018) and (Poggi *et al.*, 2000). This basically means that the current state depends only on the immediately previous state and that the states and transition probabilities do not vary over time. A state basically determines the amount of energy that is harvested by the photovoltaic cells that convert energy from the sun into a flow of electrons. In this model, we consider S states and let $\mathbf{P}$ be the square matrix of transition probabilities of order S. This matrix stores the transition probabilities $p_{x,y}$ from state x to state y with $x, y \in \{1, \ldots, S\}$. Let $E_{n,l}$ denote the amount of energy harvested at H-AP $n \in \mathcal{N}$ during a TTI $l \in \mathcal{L}$. We consider that $E_{n,l}$ is a continuous and random variable within the interval $[(s-1)(B_{\max}/S),\ s(B_{\max}/S)]$ for $s \in \{1, \ldots, S\}$. This representation of the harvested energy as a continuous random variable simulates the actual behavior of the harvested solar energy, that presents a continuous nature in practice (Carvalho *et al.*, 2018).

In order to provide QoS guarantees to the connected terminals, we consider not only the renewable energy source but also energy drawn from the electrical grid. This allows to compensate for the randomness of the energy drawn from EH sources (Aggarwal *et al.*, 2017). Therefore, the allocated power, $\rho_{n,k,l}$, is such that $\rho_{n,k,l} = \rho^{\mathrm{e}}_{n,k,l} + \rho^{\mathrm{g}}_{n,k,l}$, where $\rho^{\mathrm{e}}_{n,k,l}$ and $\rho^{\mathrm{g}}_{n,k,l}$ denote the power drawn from EH sources and the electrical grid, respectively. We also define E_{fix} for each H-AP as a constant energy quantity required to transmit information about the current battery level and received pilot signal to the central unit from the H-APs, as well as the energy consumed by the circuit. The energy from the circuit includes the power consumed by the digital to analog converters, mixers and filters. Since the H-APs are powered by both EH sources and the electrical grid, the required energy for the H-APs operation can be written as:

$$E_{\mathrm{fix}} = E^{\mathrm{e}}_{n,l} + E^{\mathrm{g}}_{n,l}, \quad \forall n \in \mathcal{N}, \forall l \in \mathcal{L}, \tag{3.2}$$

where $E^{\mathrm{e}}_{n,l}$ and $E^{\mathrm{g}}_{n,l}$ are the variable energy drawn from EH sources and the electrical grid at H-AP $n \in \mathcal{N}$ and during TTI $l \in \mathcal{L}$, respectively. Furthermore, we set in (3.3) the total energy consumed from EH sources, $E^{\mathrm{e}}_{\mathrm{total}}$, and also the total energy consumed from the electrical grid, $E^{\mathrm{g}}_{\mathrm{total}}$, during the L TTIs, respectively.

$$E^{\mathrm{e}}_{\mathrm{total}} = \tau \sum_{n\in\mathcal{N}} \sum_{k\in\mathcal{K}} \sum_{l\in\mathcal{L}} \rho^{\mathrm{e}}_{n,k,l} + \sum_{n\in\mathcal{N}} \sum_{l\in\mathcal{L}} E^{\mathrm{e}}_{n,l}, \tag{3.3a}$$

$$E^{\mathrm{g}}_{\mathrm{total}} = \tau \sum_{n\in\mathcal{N}} \sum_{k\in\mathcal{K}} \sum_{l\in\mathcal{L}} \rho^{\mathrm{g}}_{n,k,l} + NLE_{\mathrm{fix}} - \sum_{n\in\mathcal{N}} \sum_{l\in\mathcal{L}} E^{\mathrm{e}}_{n,l}. \tag{3.3b}$$

The summary of the main variables of this chapter is shown in Table 5 [2].

Tabela 5 – Summary of the main variables of chapter 3

Variable	Description
N	Number of H-APs.
K	Number of terminals.
L	Number of TTIs.
$\mathcal{N}$	Set of all H-APs.
$\mathcal{K}$	Set of all terminals.
$\mathcal{L}$	Set of all TTIs.
$\rho^{\mathrm{e}}_{n,k,l}$	Power drawn from EH sources.
$\rho^{\mathrm{g}}_{n,k,l}$	Power drawn from the electrical grid.
$\rho_{n,k,l}$	Allocated power ($\rho_{n,k,l} = \rho^{\mathrm{e}}_{n,k,l} + \rho^{\mathrm{g}}_{n,k,l}$).
$E^{e}_{n,l}$	Energy drawn from EH sources.
$E^{g}_{n,l}$	Energy drawn from the electrical grid.
E_{fix}	Constant energy quantity required for each H-AP during a given TTI.
$E_{n,l}$	Amount of energy harvested at H-AP $n \in \mathcal{N}$ during a TTI $l \in \mathcal{L}$.
$B_{\max}$	Maximal battery capacity.
$\rho_{\max}$	Maximal transmit power at each H-AP.

3.3 Problem Formulation

The aim of this chapter is to study the max-min fairness problem, where we maximize the minimum of a metric of interest given some constraints on the resources. In this chapter, we consider the SINR as the metric of interest. Furthermore, in this problem we also consider two groups of users. In the first group we have the users that require a high QoS requirement, called *gold users* and they are contained in the set $\mathcal{S} \subset \mathcal{K}$. The remaining users belong to the second group where users do not have explicity QoS requirements and are supposed to be using best effort services. However, due to the nature of the max-min fairness problem, the SINRs of the users outside the set $\mathcal{S}$ will reach the highest possible SINRs in order to increase the fairness level in the system. Roughly speaking, in the optimal solution of our problem the stringent requirements of the gold users are satisfied while the SINRs of the other users is improved as much as possible. The problem to maximize the minimum SINR of the system, in offline

[2] The variables defined in the Table 5 are valid only in this chapter.

scenarios, is shown in (3.4). As discussed in Section 1.2.5, considering an offline approach means assuming that the nodes have full knowledge of the CSI and of the amount and arrival time of the harvested energy. Offline approaches are optimistic/idealistic situations in practice, but it can provide analytical/heuristic solutions for designing the optimal transmission strategy. On the other hand, with online approaches, the nodes only have statistical knowledge of the energy harvesting process and CSI. As already discussed, note that our objective in (3.4a) is to maximize the minimum achievable SINR among all the users, thereby, providing max-min fairness. Regarding the problem constraints, in (3.4b) a minimum received SINR, denoted γ_{th}, to each gold user $k \in \mathcal{S}$ and TTI $l \in \mathcal{L}$ is guaranteed. The set of constraints (3.4c) ensure the energy causality, i.e., the consumed harvested energy at H-AP $n \in \mathcal{N}$ cannot exceed the energy harvested by it. The set of constraints (3.4d) specifies that the harvested energy at the current TTI cannot exceed the maximal battery capacity. Constraint (3.4e) mathematically states that the total energy spent in the system from the grid must be lower a fraction, ξ, from the total renewable energy. The lower the value of ξ, the less grid energy is consumed, i.e., the system operates towards self-sustainability. Our main idea with this constraint is to study the impact of limitations imposed on the energy sources consumption in the system performance. Furthermore, this constraint allows the system operators to control the proportion of consumed energy in the system in different scenarios depending on the financial cost of renewable[3] and grid energy. The set of constraints (3.4f) specifies that the transmit power at each H-AP should not exceed the limit ρ_{max} due to the limited linear range of the power amplifiers. Finally, constraints (3.4g) and

[3] Costs of renewable energy include capital costs such as installing solar cells, sitting costs that involves permits and community relations, and regulatory barriers. Operational costs of renewable energy are minimal in general.

(3.4h) ensure the non-negativity of the allocated amounts of power or energy.

$$\max_{\{\rho^{\mathrm{e}}_{n,k,l},\rho^{\mathrm{g}}_{n,k,l},E^{\mathrm{e}}_{n,l}\}} \min\left\{\gamma_{1,1},\gamma_{1,2},\ldots,\gamma_{k,l},\ldots,\gamma_{K,L}\right\}, \tag{3.4a}$$

$$\text{s.t. } \gamma_{k,l} \geq \gamma_{\text{th}}, \quad \forall k \in \mathcal{S} \subset \mathcal{K}, \forall l \in \mathcal{L}, \tag{3.4b}$$

$$\sum_{l=1}^{\tilde{l}} \left(E^{\mathrm{e}}_{n,l} + \tau \sum_{k\in\mathcal{K}} \rho^{\mathrm{e}}_{n,k,l} \right) \leq \sum_{l=1}^{\tilde{l}} E_{n,l}, \tag{3.4c}$$

$$\forall n \in \mathcal{N}, \forall \tilde{l} \in \mathcal{L},$$

$$\sum_{l=1}^{\tilde{l}} E_{n,l} - \sum_{l=1}^{\tilde{l}-1} \left(E^{\mathrm{e}}_{n,l} + \tau \sum_{k\in\mathcal{K}} \rho^{\mathrm{e}}_{n,k,l} \right) \leq B_{\max}, \tag{3.4d}$$

$$\forall n \in \mathcal{N}, \forall \tilde{l} \in \mathcal{L}\backslash\{1\},$$

$$E^{\mathrm{g}}_{\text{total}} \leq \xi E^{\mathrm{e}}_{\text{total}}, \tag{3.4e}$$

$$\sum_{k\in\mathcal{K}} (\rho^{\mathrm{e}}_{n,k,l} + \rho^{\mathrm{g}}_{n,k,l}) \leq \rho_{\max}, \quad \forall n \in \mathcal{N}, \forall l \in \mathcal{L}, \tag{3.4f}$$

$$\rho^{\mathrm{e}}_{n,k,l}, \rho^{\mathrm{g}}_{n,k,l} \geq 0, \quad \forall n \in \mathcal{N}, \forall k \in \mathcal{K}, \forall l \in \mathcal{L}, \tag{3.4g}$$

$$E_{\text{fix}} \geq E^{\mathrm{e}}_{n,l} \geq 0, \quad \forall n \in \mathcal{N}, \forall l \in \mathcal{L}. \tag{3.4h}$$

3.4 Proposed Solutions

In this section, we discuss the optimal solution to problem (3.4) presented in Section 3.3. Furthermore, we also provide an alternative approach to solve optimally this same problem.

3.4.1 Optimal Solution

Before discussing the optimal solution to problem (3.4), we introduce its matrix modeling, defining first $\mathbf{u} = [\rho^{\mathrm{g}}_{1,1,1},\ldots,\rho^{\mathrm{g}}_{N,K,L},\rho^{\mathrm{e}}_{1,1,1},\ldots,\rho^{\mathrm{e}}_{N,K,L},E^{\mathrm{e}}_{1,1},\ldots,E^{\mathrm{e}}_{N,L}]^T$ as the optimization vector of problem (3.4). Through $\mathbf{u}$, we can obtain the subvectors $\boldsymbol{\rho}^{\mathrm{g}} = [\rho^{\mathrm{g}}_{1,1,1},\ldots,\rho^{\mathrm{g}}_{N,K,L}]^T$, $\boldsymbol{\rho}^{\mathrm{e}} = [\rho^{\mathrm{e}}_{1,1,1},\ldots,\rho^{\mathrm{e}}_{N,K,L}]^T$ and $\mathbf{e}^{\mathrm{e}} = [E_{1,1},\ldots,E_{N,L}]^T$ as shown below.

$$\boldsymbol{\rho}^{\mathrm{g}} = \mathbf{P}^{\mathrm{g}}\mathbf{u}, \mathbf{P}^{\mathrm{g}} = [\mathbf{I}_{NKL}\ \mathbf{0}_{NKL}\ \mathbf{0}_{NKL\times NL}], \tag{3.5a}$$

$$\boldsymbol{\rho}^{\mathrm{e}} = \mathbf{P}^{\mathrm{e}}\mathbf{u}, \mathbf{P}^{\mathrm{e}} = [\mathbf{0}_{NKL}\ \mathbf{I}_{NKL}\ \mathbf{0}_{NKL\times NL}], \tag{3.5b}$$

$$\mathbf{e}^{\mathrm{e}} = \mathbf{E}^{\mathrm{e}}\mathbf{u}, \mathbf{E}^{\mathrm{e}} = [\mathbf{0}_{NL\times NKL}\ \mathbf{0}_{NL\times NKL}\ \mathbf{I}_{NL}]. \tag{3.5c}$$

This allows us to rewrite the linear constraints (3.4b), (3.4c), (3.4d), (3.4e), (3.4f), (3.4g) and (3.4h) as follows, respectively:

$$\frac{\left[\left[\mathbf{1}_{1\times N}\otimes\mathbf{I}_{KL}\right]\odot\left[\mathbf{1}_{KL\times 1}\otimes\left[\mathbf{1}_{1\times N}\otimes\boldsymbol{\omega}^{T}\right]\right]\right]\left(\boldsymbol{\rho}^{\mathrm{g}}+\boldsymbol{\rho}^{\mathrm{e}}\right)}{\left[\left[\mathbf{1}_{1\times N}\otimes\left[\left[\mathbf{1}_{K}-\mathbf{I}_{K}\right]\otimes\mathbf{I}_{L}\right]\right]\odot\left[\mathbf{1}_{KL\times 1}\otimes\left[\mathbf{1}_{1\times N}\otimes\boldsymbol{\omega}^{T}\right]\right]\right]\left(\boldsymbol{\rho}^{\mathrm{g}}+\boldsymbol{\rho}^{\mathrm{e}}\right)+\sigma^{2}}\geq\gamma_{\text{th}} \tag{3.6a}$$

$$\left[\mathbf{I}_{N}\otimes\mathbf{T}_{L}\right]\mathbf{e}^{\mathrm{e}}+\left[\left[\mathbf{I}_{N}\otimes\left[\mathbf{1}_{1\times K}\otimes\mathbf{T}_{L}\right]\right]\otimes\left[\tau\right]\right]\boldsymbol{\rho}^{\mathrm{e}}\leq\left[\mathbf{I}_{N}\otimes\mathbf{T}_{L}\right]\mathbf{e} \tag{3.6b}$$

$$\left[\mathbf{I}_{N}\otimes\mathbf{T}_{L}\right]\mathbf{e}-\left[\mathbf{I}_{N}\otimes{\mathbf{T}^{*}}_{L}\right]\mathbf{e}^{\mathrm{e}}-\left[\left[\mathbf{I}_{N}\otimes\left[\mathbf{1}_{1\times K}\otimes{\mathbf{T}^{*}}_{L}\right]\right]\otimes\left[\tau\right]\right]\boldsymbol{\rho}^{\mathrm{e}}\leq\mathbf{b} \tag{3.6c}$$

$$E^{\mathrm{g}}_{\text{total}}\leq\xi E^{\mathrm{e}}_{\text{total}} \tag{3.6d}$$

$$\left[\mathbf{I}_{N}\otimes\left[\mathbf{1}_{1\times K}\otimes\mathbf{I}_{L}\right]\right]\left(\boldsymbol{\rho}^{\mathrm{g}}+\boldsymbol{\rho}^{\mathrm{e}}\right)\leq\boldsymbol{\rho}_{\text{max}} \tag{3.6e}$$

$$\boldsymbol{\rho}^{\mathrm{g}},\boldsymbol{\rho}^{\mathrm{e}}\geq\mathbf{0}_{NKL\times 1}, \tag{3.6f}$$

$$\mathbf{e}_{\text{fix}}\geq\mathbf{e}^{\mathrm{e}}\geq\mathbf{0}_{NL\times 1}, \tag{3.6g}$$

where $\boldsymbol{\omega}=[\mid\mathbf{w}_1^1\mathbf{g}_1^1\mid^2,\mid\mathbf{w}_1^2\mathbf{g}_1^2\mid^2,\mid\mathbf{w}_1^3\mathbf{g}_1^3\mid^2,\ldots,\mid\mathbf{w}_K^L\mathbf{g}_K^L\mid^2]^T$, $\mathbf{e}=[E_{1,1},\ldots,E_{N,L}]^T$ and $\mathbf{T}_v$ is a $v\times v$ lower triangular matrix composed by 1's. ${\mathbf{T}^{*}}_v$ is identical to $\mathbf{T}_v$ without the last row. Moreover, $\mathbf{b}=\mathbf{1}_{N(L-1)\times 1}\otimes[B_{\text{max}}]$, $\boldsymbol{\rho}_{\text{max}}=\mathbf{1}_{NL\times 1}\otimes[\rho_{\text{max}}]$, $\mathbf{e}_{\text{fix}}=\mathbf{1}_{NL\times 1}\otimes[E_{\text{fix}}]$. $E^{\mathrm{e}}_{\text{total}}$ and $E^{\mathrm{g}}_{\text{total}}$ can be rewritten as $E^{\mathrm{e}}_{\text{total}}=[\mathbf{1}_{1\times NKL}\otimes[\tau]]\boldsymbol{\rho}^{\mathrm{e}}+[\mathbf{1}_{1\times NL}]\mathbf{e}^{\mathrm{e}}$ and $E^{\mathrm{g}}_{\text{total}}=[\mathbf{1}_{1\times NKL}\otimes[\tau]]\boldsymbol{\rho}^{\mathrm{g}}-[\mathbf{1}_{1\times NL}]\mathbf{e}^{\mathrm{e}}+NLE_{\text{fix}}$, respectively. For the sake of convenience we define again the following matrix operators $\otimes$, $\odot$ and $(\cdot)^T$ are the Kronecker product, the Hadamard product and the transpose matrix, respectively.

Given the constraints set in (3.6), we can define as $\mathcal{U}$ the domain of the optimization of problem (3.4) as shown in (3.7).

$$\mathcal{U}=\left\{\mathbf{u}\mid\boldsymbol{\Phi}\mathbf{u}\leq\boldsymbol{\mu},\ \mathbf{u}\in\mathbb{R}_{+}^{z\times 1}\right\}, \tag{3.7a}$$

$$\boldsymbol{\Phi}=\begin{bmatrix}\left[\mathbf{Q}[\mathbf{P}^{\mathrm{g}}+\mathbf{P}^{\mathrm{e}}]\right]\otimes[\gamma_{\text{th}}]-\mathbf{P}[\mathbf{P}^{\mathrm{g}}+\mathbf{P}^{\mathrm{e}}]\\ \left[\mathbf{I}_{N}\otimes\mathbf{T}_{L}\right]\mathbf{E}^{\mathrm{e}}+\left[\left[\mathbf{I}_{N}\otimes\left[\mathbf{1}_{1\times K}\otimes\mathbf{T}_{L}\right]\right]\otimes\left[\tau\right]\right]\mathbf{P}^{\mathrm{e}}\\ -\left[\mathbf{I}_{N}\otimes{\mathbf{T}^{*}}_{L}\right]\mathbf{E}^{\mathrm{e}}-\left[\left[\mathbf{I}_{N}\otimes\left[\mathbf{1}_{1\times K}\otimes{\mathbf{T}^{*}}_{L}\right]\right]\otimes\left[\tau\right]\right]\mathbf{P}^{\mathrm{e}}\\ E^{\mathrm{g}}_{\text{total}}-\xi E^{\mathrm{e}}_{\text{total}}\\ \left[\mathbf{I}_{N}\otimes\left[\mathbf{1}_{1\times K}\otimes\mathbf{I}_{L}\right]\right]\left(\mathbf{P}^{\mathrm{g}}+\mathbf{P}^{\mathrm{e}}\right)\\ -\mathbf{P}^{\mathrm{g}}\\ -\mathbf{P}^{\mathrm{e}}\\ -\mathbf{E}^{\mathrm{e}}\\ \mathbf{E}^{\mathrm{e}}\end{bmatrix},\boldsymbol{\mu}=\begin{bmatrix}\mathbf{0}_{KL\times 1}\\ \left[\mathbf{I}_{N}\otimes\mathbf{T}_{L}\right]\mathbf{e}\\ \mathbf{b}-\left[\mathbf{I}_{N}\otimes\mathbf{T}_{L}\right]\mathbf{e}\\ 0\\ \boldsymbol{\rho}_{\text{max}}\\ \mathbf{0}_{NKL\times 1}\\ \mathbf{0}_{NKL\times 1}\\ \mathbf{0}_{KL\times 1}\\ \mathbf{e}_{\text{fix}}\end{bmatrix},$$

Algoritmo 3: Generalized Dinkelbach algorithm applied in problem (3.10)

Require: $\epsilon > 0$; $i \leftarrow 0$; $\eta_i \geq 0$;
1: **while** $F(\eta_i) > \epsilon$ **do**
2: $\quad \mathbf{u}_i^\star \leftarrow \arg\max_{\mathbf{u}\in\mathcal{U}} \{\min_{k\in\mathcal{K},l\in\mathcal{L}}\{\mathtt{f}_{k,l}(\mathbf{u}) - \eta_i \mathtt{g}_{k,l}(\mathbf{u})\}\}$;
3: $\quad F(\eta_{i+1}) \leftarrow \min_{k\in\mathcal{K},l\in\mathcal{L}}\{\mathtt{f}_{k,l}(\mathbf{u}_i^\star) - \eta_i \mathtt{g}_{k,l}(\mathbf{u}_i^\star)\}$;
4: $\quad \eta_{i+1} \leftarrow \min_{k\in\mathcal{K},l\in\mathcal{L}} \{\mathtt{f}_{k,l}(\mathbf{u}_i^\star)/\mathtt{g}_{k,l}(\mathbf{u}_i^\star)\}$; $i \leftarrow i+1$;
5: **end while return** $\mathbf{u}_{i-1}^\star$;

where $z = NL(2K+1)$ and:

$$\mathbf{P} = \left[[\mathbf{1}_{1\times N} \otimes \mathbf{I}_{KL}] \odot \left[\mathbf{1}_{KL\times 1} \otimes \left[\mathbf{1}_{1\times N} \otimes \boldsymbol{\omega}^T\right]\right]\right], \tag{3.8a}$$

$$\mathbf{Q} = \left[[\mathbf{1}_{1\times N} \otimes [[\mathbf{1}_K - \mathbf{I}_K] \otimes \mathbf{I}_L]] \odot \left[\mathbf{1}_{KL\times 1} \otimes \left[\mathbf{1}_{1\times N} \otimes \boldsymbol{\omega}^T\right]\right]\right] + \sigma^2. \tag{3.8b}$$

Finally, we can rewrite SINR in (3.1) according to (3.9).

$$\gamma_{k,l} = \frac{\mathtt{f}_{k,l}(\mathbf{u})}{\mathtt{g}_{k,l}(\mathbf{u})}, \tag{3.9a}$$

$$\mathtt{f}_{k,l}(\mathbf{u}) = \mathbf{p}_{k,l}\mathbf{u}, \tag{3.9b}$$

$$\mathtt{g}_{k,l}(\mathbf{u}) = \mathbf{q}_{k,l}\mathbf{u}, \tag{3.9c}$$

where $\mathbf{p}_{k,l}$ and $\mathbf{q}_{k,l}$ are the $((k-1)L+l)$-th row of matrices $\mathbf{P}$ and $\mathbf{Q}$, respectively. Thereby, since problem (3.4) belongs to the class of generalized fractional problems we can rewrite it according to (3.10) and re-employ generalized Dinkelbach algorithm (Algorithm 3) to solve it. However, note that in this case the problem that is solved iteratively between lines 2 and 5 of Algortithm 3 is a linear programming (LP) and, therefore, it can be optimally solved employing the Karmarkar algorithm whose worst-case computational complexity is polynomial given by $\mathcal{O}((NL(2K+1))^{3.5})$ (Karmarkar, 1984).

$$\max_{\mathbf{u}\in\mathcal{U}} \min \left\{ \frac{\mathtt{f}_{1,1}(\mathbf{u})}{\mathtt{g}_{1,1}(\mathbf{u})}, \frac{\mathtt{f}_{1,2}(\mathbf{u})}{\mathtt{g}_{1,2}(\mathbf{u})}, \ldots, \frac{\mathtt{f}_{k,l}(\mathbf{u})}{\mathtt{g}_{k,l}(\mathbf{u})}, \ldots, \frac{\mathtt{f}_{K,L}(\mathbf{u})}{\mathtt{g}_{K,L}(\mathbf{u})} \right\}. \tag{3.10a}$$

3.4.2 Alternative Solution

As discussed earlier, problem (3.4) can be seen as a problem of fairness maximization and its purpose is to ensure the highest SINR floor for a given set of constraints. This reasoning is particularly interesting because we can formulate another optimization problem equivalent to problem (3.4) but that allows the search for its optimal solution following another streategy. For

Algoritmo 4: BIM-based proposed solution for problem (3.10)

Require: $\epsilon > 0$; $i \leftarrow 1$; $j \leftarrow 1$; $a_i \leftarrow 0$; $b_i \leftarrow \gamma_{\text{th}}$; $\Theta \leftarrow \emptyset$;
1: **while** $b_i - a_i > \epsilon$ **do**
2: set $\varepsilon_i \leftarrow (a_i + b_i)/2$;
3: **if** problem (3.11) is feasible **then**
4: $\theta_j \leftarrow \varepsilon_i; \Theta \leftarrow \Theta \cup \{\theta_j\}; j \leftarrow j + 1$;
5: $i \leftarrow i + 1; a_i \leftarrow (a_i + b_i)/2; b_i \leftarrow b_{i-1}$;
6: **else**
7: $i \leftarrow i + 1; b_i \leftarrow (a_i + b_i)/2; a_i \leftarrow a_{i-1}$;
8: **end if**
9: **end while return** Θ;

this, we present the *feasibility problem* in (3.11), where it is an LP for a specific value of $\varepsilon \in \mathbb{R}$. We can demonstrate that through (3.11) it is possible to find the highest value of ε searching it in a given interval following a processing based on the bisection method (BIM). This result is presented in Proposition 4.

$$\underset{\mathbf{u}\in\mathcal{U}}{\text{find}}\ \mathbf{u}, \tag{3.11a}$$

$$\text{s.t. } \gamma_{k,l}(\mathbf{u}) \geq \varepsilon, \quad \forall k \in \mathcal{K}, \forall l \in \mathcal{L}. \tag{3.11b}$$

Proposition 4. *Let $\varepsilon^\star$ be the highest value such that $\gamma_{k,l} \geq \varepsilon^\star$, $\forall k \in \mathcal{K}, \forall l \in \mathcal{L}$ for the optimal solution of problem* (3.10) *by Algorithm 3. Assuming that $\varepsilon^\star \in [a_1, b_1]$, then it is possible to find $\varepsilon^\star$ through a sequence of feasibility tests on the constraints in problem* (3.11) *by changing ε according to the bisection method.*

Demonstração. Suppose $\varepsilon^\star \in I_1 = [a_1, b_1]$ such that $a_1 \leq \varepsilon^\star, \varepsilon_1 \leq b_1$ and an initial guess for ε_1 as $\varepsilon_1 = \frac{a_1+b_1}{2}$. If problem (3.11) is feasible for ε_1 then $I_2 = [a_2, b_2]$ with $a_2 = \frac{a_1+b_1}{2}$ and $b_2 = b_1$. If infeasible, we have that $b_2 = \frac{a_1+b_1}{2}$ and $a_2 = a_1$. In any case, we now have $\varepsilon_2 = \frac{a_2+b_2}{2}$ and $I_1 \supset I_2$ such that $b_2 - a_2 = \frac{1}{2}(b_1 - a_1)$ with again $a_2 \leq \varepsilon^\star, \varepsilon_2 \leq b_2$ since we are intuitively back at the start but with a smaller interval. Continuing the process by induction, we have at the i-th iteration $I_1 \supset I_2 \supset I_3 \supset I_4 \cdots I_{i-1} \supset I_i$ and $b_i - a_i = \frac{1}{2^{i-1}}(b_1 - a_1)$ with $\varepsilon_i = \frac{a_i+b_i}{2}$ such that $a_i \leq \varepsilon^\star, \varepsilon_i \leq b_i$. Now, making $i \to \infty$, we have $\lim_{i\to\infty} b_i - \lim_{i\to\infty} a_i = \lim_{i\to\infty} \frac{1}{2^{i-1}}(b_1 - a_1) \to 0$ so that $\varepsilon^\star$ and $\varepsilon_i \in \cap_{i=1}^{\infty} I_i$. Hence, since $\lim_{i\to\infty} a_i = \lim_{i\to\infty} b_i$ then it implies $\lim_{i\to\infty} a_i = \lim_{i=\infty} b_i = \lim_{i\to\infty} \varepsilon_i = \varepsilon^\star$. The proof is complete. □

Proposition 4 leads to Algorithm 4. The basic idea of this algorithm is to repeatedly bisect a given starting range and then select a subinterval where the value of $\varepsilon^\star$ must lie for

further processing. This procedure is based on BIM. Moreover, the choice of subinterval is due to the feasibility of problem (3.11) for a given value of ε_i at the i-th iteration, i.e., the optimal solution of problem (3.11) does not necessarily matter[4]. Finally, Algorithm 4 returns the set $\Theta = \{\theta_1, \theta_2, \ldots, \theta_j, \ldots\}$ with all the values of θ_j that make problem (3.11) feasible and note that exactly $\lceil \log_2((b_1 - a_1)/\epsilon) \rceil$ iterations are required before it terminates. However, strictly speaking, the optimal solution of problem (3.10) could only be obtained when $j \to \infty$. Given that the feasibility of problem (3.11) can be determined employing Karmarkar algorithm, the worst-case computational complexity of Algorithm 4 is also $\mathcal{O}((NL(2K+1))^{3.5})$.

3.5 Simulation Results

In this section, we evaluate the proposed solution (Algorithm 4) and compare it with the optimal solution (Algorithm 3). We firstly present the simulation parameters and, after that, the results and discussions are presented.

3.5.1 Parameters and Simulation Characteristics

Tabela 6 – Simulation parameters.

Parameter	Value
Number of H-APs	$50 - 100$
Number of terminals	$4 - 12$
Number of TTIs	5
Duration of TTI	1 ms
Outer circle radius	500 m
Inner circle radius	50 m
γ_{th}	$6 - 22$ dB
ρ_{max}	1 W
ξ	$1 - 1.15$
Bandwidth	5 Mhz
Noise power spectral density	-174 dBm/Hz

In our scenario we consider two concentric circular areas with radius r and R with $r < R$. N H-APs are uniformly distributed in the inner circle (with radius r) while terminals

[4] A feasible solution for a system of linear inequalities can be found employing, e.g, the relaxation method, introduced by Agmon (Agmon, 1954) and Motzkin and Schoenberg (Motzkin; Schoenberg, 1954). In literature there are many different versions of this method such as (Telgen, 1982), where it is generalized to handle also the infeasibility of systems. Furthermore, in (Basu *et al.*, 2013) is discussed another method recently proposed by Chubanov that is also useful for determining the feasibility of a linear problem. However, in practice, knowing if problem (3.11) for a given ε is feasible can be done simply by searching for its optimal solution employing algorithms of low computational complexity such as Karmarkar algorithm.

Figura 11 – Minimum SINR (dB) versus number of iterations of Algorithm 3 for different values of N.

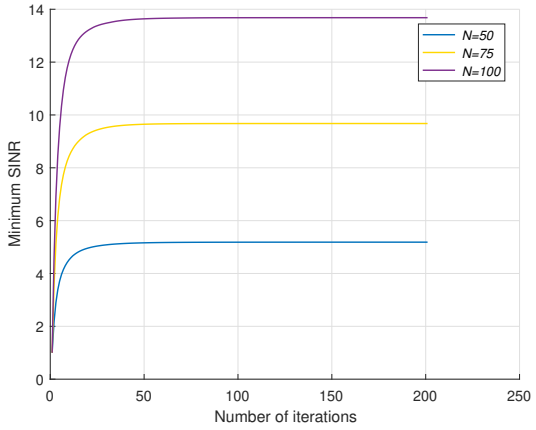

Fonte: Created by the author.

Figura 12 – Minimum SINR (dB) and average SINR (dB) versus the number of terminals.

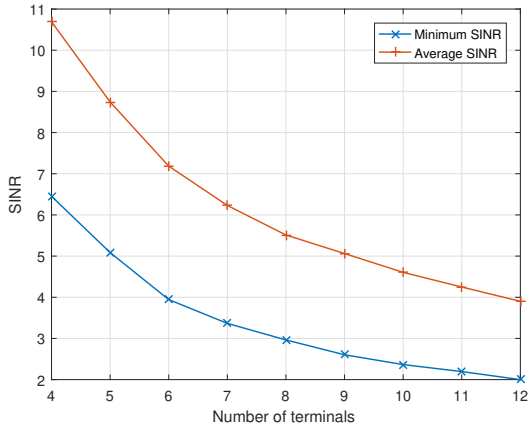

Fonte: Created by the author.

are uniformly distributed in the larger circular coverage area (with radius R). Both scenario and channel model used in this chapter are similar to the one employed in (Hamdi *et al.*, 2017). In addition, our EH model is based on the works (Carvalho *et al.*, 2018) and (Poggi *et al.*, 2000). Table 6 summarizes the main simulation parameters.

3.5.2 Discussion

Figure 11 shows the minimum SINR versus the number of iterations of Algorithm 3, considering 50, 75 and 100 antennas in the considered scenario. Although the number of antennas varies, we keep constant the total power in the system so that it does not impact the results. In addition, the number of terminals is also kept fixed. Firstly, it is possible to observe the convergence of Algorithm 3 to the optimal solution of problem (3.4). Another point to be highlighted is the important impact of varying the number of antennas that is capable of significantly increasing the SINR floor, ensuring a better link quality to all terminals and, consequently, a higher fairness level between them. Thanks to improved beamforming performance due to the increase in the number of antennas in the system, it is possible to obtain SINR gains without the need to increase the power consumption accordingly.

We also keep constant the total power as well as the number of antennas in Figure 12 and we plot average SINR and minimum SINR versus the number of terminals. As it can be seen, increasing the number of terminals an opposite effect compared with the increase in the number

Figura 13 – Jain's fairness index obtained from the optimal solution of problem (3.4) versus γ_{th} (dB).

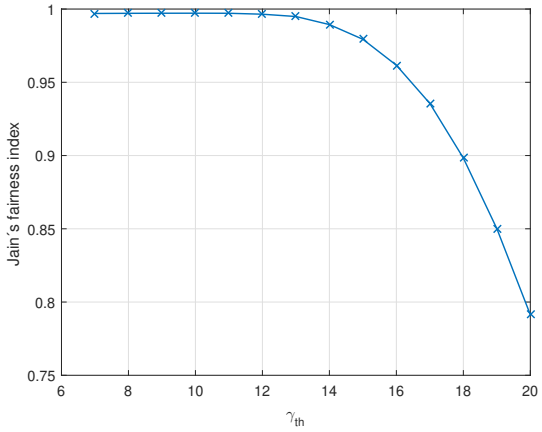

Fonte: Created by the author.

Figura 14 – Minimum SINR (dB) versus number of iterations of Algorithm 3 for different initial values of η.

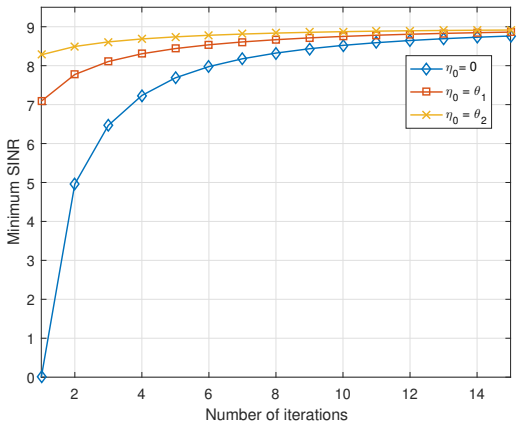

Fonte: Created by the author.

of antennas, i.e., the more terminals in the system, the lower the SINR floor and, consequently, the lower the average SINR as well. As both total power and the number of antennas are fixed and as the QoS of gold users is a strict requirement, less radio resources are left for the other users leading to a lower SINR floor.

The fairness level is analyzed employing the Jain's fairness index applied to the SINRs shown in equation (3.1). Therefore, the Jain's fairness index is given by $I(\gamma_{1,1}, \ldots, \gamma_{K,L}) = \frac{\left(\sum_{\forall k \in \mathcal{K}} \sum_{\forall l \in \mathcal{L}} \gamma_{k,l}\right)^2}{KL \sum_{\forall k \in \mathcal{K}} \sum_{\forall l \in \mathcal{L}} \gamma_{k,l}^2}$ with values in the interval $[\frac{1}{KL}, 1]$. Thus, we plot in Figure 13 $I(\gamma_{1,1}, \ldots, \gamma_{K,L})$ versus γ_{th} (SINR threshold for gold users). It is possible to note a high fairness level for low thresholds of γ_{th}, but this level tends to decrease as γ_{th} increases. Indeed, this is expected because as we increase the QoS requirements of the group $\mathcal{S}$, more resources need to be allocated to gold users decreasing the SINR floor in the system (minimum user SINR) and, thus, decreasing the fairness level. The increase in γ_{th} produces the same behaviour to the increase in the number of terminals as explained in Figure 12.

The convergence shown in Figure 11 can be speed-up and to explain this we plot again in Figure 14 the minimum SINR versus number of iterations of Algorithm 3. However, in this plot we consider three different initial values of η. In this figure, θ_1 and θ_2 $(\theta_2 > \theta_1)$ are obtained from the set Θ that is returned by Algorithm 4, i.e., θ_1 is the first value found that makes problem (3.11) feasible θ_2 is the second one, and so on. In this result, we highlight the relevance of the set Θ returned by Algorithm 4 since the values contained in this set can be used as initial thresholds for Algorithm 3 so that its convergence can be reached more rapidly. This result is

Figura 15 – Performance loss to the optimal solution (%) versus the number of iterations of BIM-based proposed solution (Algorithm 4).

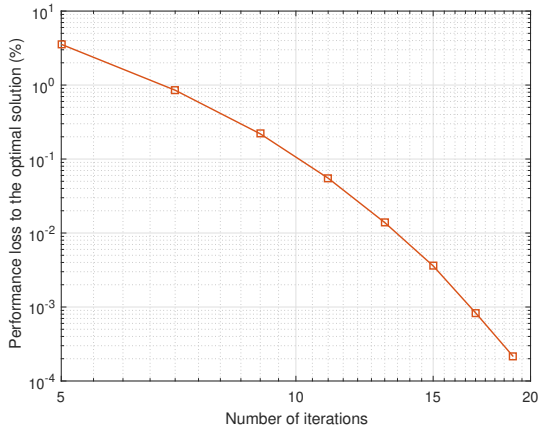

Fonte: Created by the author.

Figura 16 – Ratio between grid energy and harvested energy versus the number of iterations of BIM-based proposed solution (Algorithm 4).

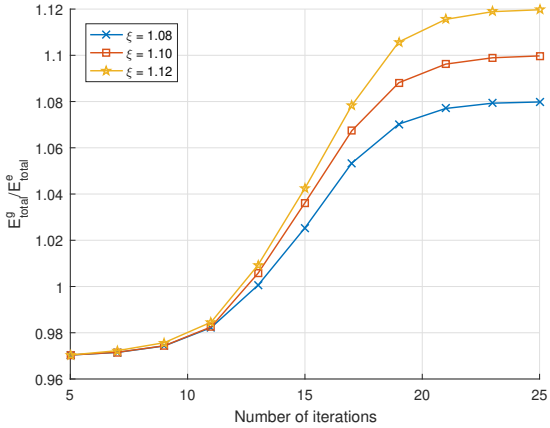

Fonte: Created by the author.

particularly interesting since Algorithm 4 can both improve the performance of Algorithm 3 and can also find an optimal solution for problem (3.4) according to Proposition 4.

The performance loss to the optimal solution versus the number of iterations of BIM-based proposed solution (Algorithm 4) is plotted in Figure 15. As it can be seen, the decreasing behavior of the error curve shown in this figure shows the convergence of the solution obtained from Algorithm 4 to the optimal solution of problem (3.4). As an example, with 10 iterations, the performance loss to the optimal solution is only $10^{-1}\%$. The convergence of Algorithm 4 to the optimal solution can also be seen from another point of view in Figure 16, which shows the ratio $E^{\mathrm{g}}_{\mathrm{total}}/E^{\mathrm{e}}_{\mathrm{total}}$ for different values of ξ versus the number of iterations of Algorithm 4. This energy ratio is related to constraint (3.4e) from problem (3.4). As the aim of problem (3.4) is to ensure the maximum SINR floor and assuming a good spatial multiplexing capacity of MRT in massive MIMO regime, in general the constraint (3.4e) is satisfied with equality. This behavior is seen in Figure 15 where we show the convergence in terms of consumed energy of ratio $E^{\mathrm{g}}_{\mathrm{total}}/E^{\mathrm{e}}_{\mathrm{total}}$ to ξ. The progressive increase in energy consumption occurs due to the value ε that also increases during the iterations of Algorithm 4, demanding, therefore, more energy. Based on that, note that Figures 15 and 16 show that although there is a performance loss to the optimal solution for low values of the number of iterations of Algorithm 4, in contrast, there is also less energy consumed from the electrical grid for the same number of iterations. As it can be seen in Figure 16 with up to 11 iterations of the algorithm 4 we have a ratio $E^{\mathrm{g}}_{\mathrm{total}}/E^{\mathrm{e}}_{\mathrm{total}} < 1$ which means that

Figura 17 – Outage probability versus γ_{th} (dB) for the solutions obtained from the optimal solution (Algorithm 3) and BIM-based proposed solution configured to 30 iterations (Algorithm 4).

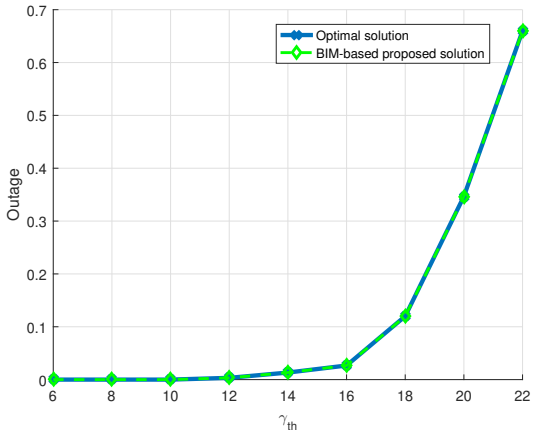

Fonte: Created by the author.

Figura 18 – Outage probability versus ξ for the solutions obtained from the optimal solution (Algorithm 3) and BIM-based proposed solution configured to 30 iterations (Algorithm 4).

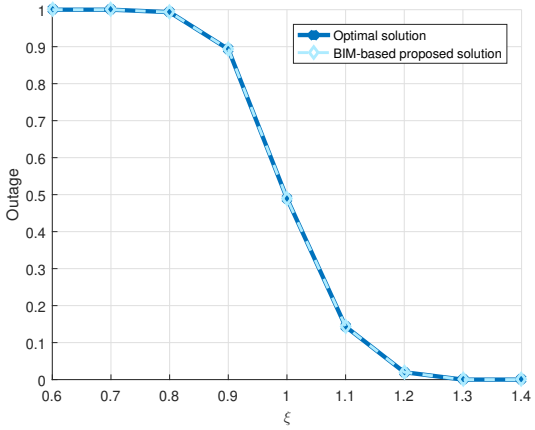

Fonte: Created by the author.

the system consumes more renewable energy than the grid energy and according to Figure 15 the performance loss to the optimal solution for that iteration number is less than $10^{-1}\%$. In other words, it is possible to make the system more sustainable in exchange for a very small performance loss. Therefore, through more careful power optimization and realizing a trade-off between performance loss and energy consumption, less energy from the electrical grid can be consumed employing the proposed solution.

The performance of Algorithms 3 and 4 in terms of outage probability versus γ_{th} and ξ is plotted in Figs. 17 and 18, respectively. In Figure 17 we consider an outage a situation where constraint (3.4b) cannot be met, whereas for Figure 18 an outage is when constraint (3.4e) is violated. Despite the similar performance of Algorithms 3 and 4 in terms of outage probability, according to Figures 13 and 17, the increase of γ_{th} can both decrease the fairness level in the system and lead to a rise in the outage rate so that the QoS requirement of gold users can become a bottleneck to the system. Now, regarding Figure 18, note that the variable ξ also has an important impact on the system performance in terms of outage. This is because ξ imposes a limit on the energy consumption, i.e., the amount of energy drawn from the electrical grid depends directly on ξ and, therefore, its value can compromise QoS satisfaction as well as system operation. However, as previously explained, the variable ξ also is an important tool for

the system operators since they can adjust the proportion of consumed energy between the grid and renewable depending on different factor such as the capital and operational costs to use each energy source.

3.6 Partial Conclusions

In this chapter, we investigated the max-min fairness problem in an energy-harvesting-aided distributed massive MIMO system. In order to provide fairness in the system we maximized the minimum SINR in offline scenarios ensuring also QoS constraints. We also modeled a constraint where the total consumed energy between the grid and renewable sources should keep a certain proportion. This problem resulted in a generalized fractional programming problem that was solved optimally using generalizations of Dinkelbach's approach to fractional problems. Moreover, we also provided an alternative solution to this same problem based on the bisection method. In the results we showed firstly that the optimal solution quickly converges to the optimal solution depending on the initialization of the algorithm. Furthermore, we showed that the solution based on the bisection method is also able to approximate the optimal solution in more iterations and offering an interesting trade-off between energy consumption and performance loss to optimal solution. Finally, we presented the impact of variable such as user QoS and energy proportion on the the fairness level and outage rate.

4 CONCLUSIONS AND FUTURE WORK

Along this master's thesis we basically dealt with QoS-constrained RRA on cooperative networks and on massive MIMO systems. Cooperative networks and massive MIMO are important technologies for 4G and 5G systems. Our goal was to investigate issues related to EE and fairness, proposing simplifications or alternative solutions to the problems addressed in each chapter. A general summary of each chapter is shown below.

In Chapter 1, we presented the important concepts related to the development of the following chapters. In this way, we addressed fundamental concepts about OFDM and OFDMA, RRA, cooperative networks, massive MIMO systems and EH technology. Besides, we discussed several papers correlated to our work and presented our main contributions.

In Chapter 2, we investigated RRA as three optimization problems in the context of EE in cooperative OFDMA networks with multiple relays and multiple node destinations. These problems include the problems of total power minimization, total EE maximization, and finally minimum individual EE maximization. This resulted in fractional and linear non-convex combinatorial problems that were duly formulated and simplified through a property that exploits the employment of the DF protocol present in the relays. Then, their respective optimal algorithms/methods and computational complexities were presented. The provided optimal solutions to the fractional-nature problems were based on Dinkelbach's classical and generalized approach. In the results, we showed the convergence to optimal solution of the proposed algorithms and gains in terms of total EE as we increase the number of relays in the system. In addition, we showed that the problems of power minimization and EE maximization converge to the same total EE as we increase the data rate requirements at the destination nodes. Indeed, this is an important result because it illustrates that the maximization of the total EE can be achieved more easily in some scenarios. Finally, we investigated the problem of maximizing the minimum individual EE and we validated that it is capable of providing high fairness level in the system in terms of EE. Moreover, we showed that the problems of EE maximization and minimum individual EE maximization also tend to converge to the same total EE when high data rate requirements are required.

In Chapter 3, we considered an EH-aided distributed massive MIMO system in an offline scenario and we investigated RRA as a max-min fairness problem. Thereby, we formulated an optimization problem with power/energy allocation in order to maximize fairness in terms of SINR given the constraints on resources. As the formulated problem belongs

to the class of generalized fractional programming problems, its optimal solution was again achieved through Dinkelbach's generalized approach. However, we also provided an alternative solution based on the bisection method to solve this problem optimally. We also discussed the computational complexities of the proposed solutions. In the results, we firstly showed that as we increase the number of antennas at the transmitter the system performance in terms of minimum SINR increases considerably even with the use of simple beamforming techniques such as MRT. Moreover, we discussed on fairness-oriented resource allocation and we evaluated the performance of the proposed solutions. Thereby, we showed that our proposed solution based on the bisection method is able to converge to optimal solution in a few iterations. Besides, that solution is also able to speed-up the convergence of the generalized Dinkelbach algorithm and offering an interesting trade-off between energy consumption and loss of performance to optimal solution as was discussed. Finally, we also investigated the performance of the system in terms of outage rate with respect to users QoS and the limitation of grid energy.

Lastly, the work developed in this master's thesis can open new research directions to be investigated. For Chapter 2 efficient solutions with low computational cost can be provided for the problems presented therein. Moreover, considering different scenarios by varying, for example, the relative distances between the nodes of the current scenario can also be investigated in the future. This may give rise to new and interesting trade-offs related to EE and fairness. Regarding Chapter 3, considering imperfect CSI and investigating online scenarios can be appealing for future research. However, although this leads to a more realistic mathematical formulation of the problem, it can also bring more complexity in terms of optimal/heuristic solutions. Another interesting possibility is to integrate promising technologies for the 5G such as Full-Duplex and nonorthogonal multiple access (NOMA) into the problem. Moreover, note that in both Chapter 2 and Chapter 3, the RRA problems were proposed to work only over downlink transmissions. Therefore, in future works, the solutions proposed in this thesis could be adapted to uplink transmissions.

BIBLIOGRAPHY

Aggarwal, V.; Bell, M. R.; Elgabli, A.; Wang, X.; Zhong, S. Joint energy-bandwidth allocation for multiuser channels with cooperating hybrid energy nodes. **IEEE Transactions on Vehicular Technology**, IEEE, v. 66, n. 11, p. 9880–9889, 2017.

Agmon, S. The relaxation method for linear inequalities. **Canadian Journal of Mathematics**, Cambridge University Press, v. 6, p. 382–392, 1954.

Ahmed, I.; Butt, M. M.; Psomas, C.; Mohamed, A.; Krikidis, I.; Guizani, M. Survey on energy harvesting wireless communications: Challenges and opportunities for radio resource allocation. **Computer Networks**, Elsevier, v. 88, p. 234–248, 2015.

Anzai, Y. On integer fractional programming. **Journal of the Operations Research Society of Japan**, v. 17, n. 1, p. 49–66, 1974.

Arash, M.; Yazdian, E.; Fazel, M. S.; Brante, G.; Imran, M. A. Employing antenna selection to improve energy efficiency in massive MIMO systems. **Transactions on Emerging Telecommunications Technologies**, Wiley Online Library, v. 28, n. 12, p. e3212, 2017.

Basu, A.; Loera, J. A. D.; Junod, M. On chubanov's method for linear programming. **Informs journal on computing**, INFORMS, v. 26, n. 2, p. 336–350, 2013.

Blasco, P.; Gunduz, D.; Dohler, M. A learning theoretic approach to energy harvesting communication system optimization. **IEEE Transactions on Wireless Communications**, IEEE, v. 12, n. 4, p. 1872–1882, 2013.

Browning, C.; Farhang, A.; Saljoghei, A.; Marchetti, N.; Vujicic, V.; Doyle, L.; Barry, L. 5G wireless and wired convergence in a passive optical network using UF-OFDM and GFDM. **arXiv preprint arXiv:1703.01956**, 2017.

Carvalho, J. A. de; Lima, F. R. M.; Maciel, T. F.; Cavalcanti, F. R. P. Radio resource allocation with QoS constraints in energy harvesting and hybrid power systems. **Journal of Communication and Information Systems**, v. 33, n. 1, 2018.

Chang, R.; Gibby, R. A theoretical study of performance of an orthogonal multiplexing data transmission scheme. **IEEE transactions on Communication Technology**, IEEE, v. 16, n. 4, p. 529–540, 1968.

Chen, H.; Huang, L.; Kumar, S.; Kuo, C. J. **Radio resource management for multimedia QoS support in wireless networks**. [S.l.]: Springer Science & Business Media, 2012.

Chen, T.; Kim, H.; Yang, Y. Energy efficiency metrics for green wireless communications. In: IEEE. **Wireless Communications and Signal Processing (WCSP), 2010 International Conference on**. [S.l.], 2010. p. 1–6.

Chen, Y.; Guo, Z.; Yang, X.; Hu, Y.; Zhu, Q. Optimization of coverage in 5G self-organizing small cell networks. **Mobile Networks and Applications**, Springer, p. 1–11, 2017.

Consortium, E. *et al.* Overview of ICT energy consumption (d8. 1). **Report FP7-2888021, European Network of Excellence in Internet Science**, 2013.

Crouzeix, J.-P.; Ferland, J. A. Algorithms for generalized fractional programming. **Mathematical Programming**, Springer, v. 52, n. 1-3, p. 191–207, 1991.

Dang, W.; Tao, M.; Mu, H.; Huang, J. Subcarrier-pair based resource allocation for cooperative multi-relay OFDM systems. **IEEE Transactions on Wireless Communications**, IEEE, v. 9, n. 5, 2010.

Dinkelbach, W. On nonlinear fractional programming. **Management science**, INFORMS, v. 13, n. 7, p. 492–498, 1967.

D'Oro, S.; Zappone, A.; Palazzo, S.; Lops, M. A learning-based approach to energy efficiency maximization in wireless networks. In: IEEE. **Wireless Communications and Networking Conference (WCNC), 2018 IEEE**. [S.l.], 2018. p. 1–6.

Ericsson. Ericsson Mobility Report. **White Paper**, 2019.

Gelenbe, E.; Caseau, Y. The impact of information technology on energy consumption and carbon emissions. **Ubiquity**, ACM, v. 2015, n. June, p. 1, 2015.

Gross, J.; Bohge, M. Dynamic mechanisms in ofdm wireless systems: A survey on mathematical and system engineering contributions. **TU-Berlin, Tech. Rep. TKN-06-001**, 2006.

Hamdi, R.; Ajib, W. Sum-rate maximizing in downlink massive MIMO systems with circuit power consumption. In: IEEE. **Wireless and Mobile Computing, Networking and Communications (WiMob), 2015 IEEE 11th International Conference on**. [S.l.], 2015. p. 437–442.

Hamdi, R.; Driouch, E.; Ajib, W. Energy management in hybrid energy large-scale mimo systems. **IEEE Transactions on Vehicular Technology**, IEEE, v. 66, n. 11, p. 10183–10193, 2017.

Host-Madsen, A.; Zhang, J. Capacity bounds and power allocation for wireless relay channels. **IEEE transactions on Information Theory**, IEEE, v. 51, n. 6, p. 2020–2040, 2005.

Hu, B.-b.; Liu, Y.-a.; Gang, X.; Gao, J.-c.; Yang, Y.-l. Energy efficiency of massive MIMO wireless communication systems with antenna selection. **The Journal of China Universities of Posts and Telecommunications**, Elsevier, v. 21, n. 6, p. 1–8, 2014.

Huaizhou, S.; Prasad, R. V.; Onur, E.; Niemegeers, I. Fairness in wireless networks: Issues, measures and challenges. **IEEE Communications Surveys & Tutorials**, IEEE, v. 16, n. 1, p. 5–24, 2014.

ITU-R Rec. M.2083. **IMT Vision–Framework and overall objectives of the future development of IMT for 2020 and beyond**. Tech. Rep. 4, 2015.

Jagannathan, R. On some properties of programming problems in parametric form pertaining to fractional programming. **Management Science**, INFORMS, v. 12, n. 7, p. 609–615, 1966.

Jain, R. K.; Chiu, D.-M. W.; Hawe, W. R. A quantitative measure of fairness and discrimination. **Eastern Research Laboratory, Digital Equipment Corporation, Hudson, MA**, 1984.

Jangsher, S.; Zhou, H.; Li, V. O.; Leung, K.-C. Joint allocation of resource blocks, power, and energy-harvesting relays in cellular networks. **IEEE Journal on Selected Areas in Communications**, IEEE, v. 33, n. 3, p. 482–495, 2015.

Jiang, D.; Zheng, H.; Tang, D.; Tang, Y. Relay selection and power allocation for cognitive energy harvesting two-way relaying networks. In: IEEE. **Electronics Information and Emergency Communication (ICEIEC), 2015 5th International Conference on**. [S.l.], 2015. p. 163–166.

Karmarkar, N. A new polynomial-time algorithm for linear programming. In: ACM. **Proceedings of the sixteenth annual ACM symposium on Theory of computing**. [S.l.], 1984. p. 302–311.

Ku, M.-L.; LI, W.; Chen, Y.; Liu, K. R. Advances in energy harvesting communications: Past, present, and future challenges. **IEEE Communications Surveys & Tutorials**, IEEE, v. 18, n. 2, p. 1384–1412, 2015.

Kuang, Y.; Zhao, L.; Zhao, H. Efficiency and fairness of energy broadcasting systems with centralized massive MIMO. In: IEEE. **2017 IEEE/CIC International Conference on Communications in China (ICCC)**. [S.l.], 2017. p. 1–5.

Lawler, E. L.; Wood, D. E. Branch-and-bound methods: A survey. **Operations research**, INFORMS, v. 14, n. 4, p. 699–719, 1966.

Li, G. Y.; Xu, Z.; Xiong, C.; Yang, C.; Zhang, S.; Chen, Y.; Xu, S. Energy-efficient wireless communications: tutorial, survey, and open issues. **IEEE Wireless Communications**, IEEE, v. 18, n. 6, 2011.

Li, Y.; Sheng, M.; Tan, C. W.; Zhang, Y.; Sun, Y.; Wang, X.; Shi, Y.; Li, J. Energy-efficient subcarrier assignment and power allocation in OFDMA systems with max-min fairness guarantees. **IEEE Transactions on Communications**, IEEE, v. 63, n. 9, p. 3183–3195, 2015.

Lima, F. R. M.; Maciel, T. F.; Cavalcanti, F. R. P. Radio resource allocation in SC-FDMA uplink with resource adjacency constraints. **Journal of Communication and Information Systems**, v. 31, n. 1, 2016.

Liu, Z.; Du, W.; Sun, D. Energy and spectral efficiency tradeoff for massive MIMO systems with transmit antenna selection. **IEEE Transactions on Vehicular Technology**, IEEE, v. 66, n. 5, p. 4453–4457, 2017.

Lu, L.; LI, G. Y.; Swindlehurst, A. L.; Ashikhmin, A.; Zhang, R. An overview of massive mimo: Benefits and challenges. **IEEE journal of selected topics in signal processing**, IEEE, v. 8, n. 5, p. 742–758, 2014.

Marzetta, T. L. Noncooperative cellular wireless with unlimited numbers of base station antennas. **IEEE Transactions on Wireless Communications**, v. 9, n. 11, p. 3590, 2010.

Marzetta, T. L.; Yang, H. **Fundamentals of massive MIMO**. [S.l.]: Cambridge University Press, 2016.

Masoudi, M.; Zaefarani, H.; Mohammadi, A.; Cavdar, C. Energy efficient resource allocation in two-tier OFDMA networks with QoS guarantees. **Wireless Networks**, Springer, v. 24, n. 5, p. 1841–1855, 2018.

Ming, Z.; Jing, Z.; Wuyang, Z.; Jinkang, Z.; Sihai, Z. Energy efficiency optimization in relay-assisted networks with energy harvesting relay constraints. **China Communications**, IEEE, v. 12, n. 2, p. 84–94, 2015.

Motzkin, T. S.; Schoenberg, I. J. The relaxation method for linear inequalities. **Canadian Journal of Mathematics**, Cambridge University Press, v. 6, p. 393–404, 1954.

Nasir, A. A.; Zhou, X.; Durrani, S.; Kennedy, R. A. Relaying protocols for wireless energy harvesting and information processing. **IEEE Transactions on Wireless Communications**, IEEE, v. 12, n. 7, p. 3622–3636, 2013.

Ng, T. C.-Y.; Yu, W. Joint optimization of relay strategies and resource allocations in cooperative cellular networks. **IEEE Journal on Selected areas in Communications**, IEEE, v. 25, n. 2, p. 328–339, 2007.

Ngo, H. **Massive MIMO: Fundamentals and system designs (Vol. 1642)**. [S.l.]: Linköping: Linköping University Electronic Press, 2015.

Ngo, H. Q.; Ashikhmin, A.; Yang, H.; Larsson, E. G.; Marzetta, T. L. Cell-free massive MIMO versus small cells. **IEEE Transactions on Wireless Communications**, IEEE, v. 16, n. 3, p. 1834–1850, 2017.

Nguyen, K.-G.; Tran, L.-N.; Tervo, O.; Vu, Q.-D.; Juntti, M. Achieving energy efficiency fairness in multicell MISO downlink. **IEEE Communications Letters**, IEEE, v. 19, n. 8, p. 1426–1429, 2015.

Poggi, P.; Notton, G.; Muselli, M.; Louche, A. Stochastic study of hourly total solar radiation in corsica using a markov model. **International journal of climatology**, Wiley Online Library, v. 20, n. 14, p. 1843–1860, 2000.

Saraiva, J. V.; Lima, F. R. M.; Maciel, T. F.; Cavalcanti, F. R. P. Relay selection, subcarrier pairing and power allocation for energy efficiency and QoS guarantees. In: IEEE. **Wireless Communications and Networking Conference (WCNC), 2018 IEEE**. [S.l.], 2018. p. 1–6.

Sheng, Z.; Fan, J.; Liu, C. H.; Leung, V. C.; Liu, X.; Leung, K. K. Energy-efficient relay selection for cooperative relaying in wireless multimedia networks. **IEEE Transactions on Vehicular Technology**, IEEE, v. 64, n. 3, p. 1156–1170, 2015.

Silva, J. M.; Silva, Y. C.; Maciel, T. F.; Cavalcanti, F. R.; Rodrigues, C. D.; Neto, M. B. C. Power allocation schemes for multichannel two-hop relaying systems. In: IEEE. **Wireless Communication Systems (ISWCS), 2012 International Symposium on**. [S.l.], 2012. p. 356–360.

Singh, K.; Gupta, A.; Ratnarajah, T. A utility-based joint subcarrier and power allocation for green communications in multi-user two-way regenerative relay networks. **IEEE Transactions on Communications**, IEEE, v. 65, n. 9, p. 3705–3722, 2017.

Singh, V. P.; Chaturvedi, A. K. Max–min fairness based linear transceiver–relay design for MIMO interference relay channel. **IET Communications**, IET, v. 11, n. 9, p. 1485–1496, 2017.

Sokun, H. U.; Bedeer, E.; Gohary, R. H.; Yanikomeroglu, H. Fairness-oriented resource allocation for energy efficiency optimization in uplink OFDMA networks. In: IEEE. **2018 IEEE Wireless Communications and Networking Conference (WCNC)**. [S.l.], 2018. p. 1–6.

Song, X.; Xu, S. Joint optimal power allocation and relay selection in full-duplex energy harvesting relay networks. In: IEEE. **2018 10th International Conference on Communication Software and Networks (ICCSN)**. [S.l.], 2018. p. 80–84.

Song, Z.; Ni, Q.; Navaie, K.; Hou, S.; Wu, S.; Sun, X. On the spectral-energy efficiency and rate fairness tradeoff in relay-aided cooperative OFDMA systems. **IEEE Transactions on Wireless Communications**, IEEE, v. 15, n. 9, p. 6342–6355, 2016.

Souza, A. R. C.; Amazonas, J. R. de A.; Abrão, T. Power and subcarrier allocation strategies for energy-efficient uplink OFDMA systems. **IEEE Journal on Selected Areas in Communications**, IEEE, v. 34, n. 12, p. 3142–3156, 2016.

Sun, W.; Li, L.; Yang, W.; Song, L. Joint subcarrier pairing, relay selection and power allocation in OFDM relay systems. In: IEEE. **Communications (ICC), 2011 IEEE International Conference on**. [S.l.], 2011. p. 1–5.

Tao, X.; Xu, X.; Cui, Q. An overview of cooperative communications. **IEEE Communications Magazine**, IEEE, v. 50, n. 6, 2012.

Telgen, J. On relaxation methods for systems of linear inequalities. **European Journal of Operational Research**, Elsevier, v. 9, n. 2, p. 184–189, 1982.

Tutuncuoglu, K.; Yener, A. Optimal power policy for energy harvesting transmitters with inefficient energy storage. In: **CISS**. [S.l.: s.n.], 2012. p. 1–6.

Ulukus, S.; Yener, A.; Erkip, E.; Simeone, O.; Zorzi, M.; Grover, P.; Huang, K. Energy harvesting wireless communications: A review of recent advances. **IEEE Journal on Selected Areas in Communications**, IEEE, v. 33, n. 3, p. 360–381, 2015.

Wang, T.; Ma, C.; Sun, Y.; Zhang, S.; Wu, Y. Energy efficiency maximized resource allocation for opportunistic relay-aided OFDMA downlink with subcarrier pairing. **Wireless Communications and Mobile Computing**, Hindawi, v. 2018, 2018.

Yu, W.; Musavian, L.; Ni, Q. Tradeoff analysis and joint optimization of link-layer energy efficiency and effective capacity toward green communications. **IEEE Transactions on Wireless Communications**, IEEE, v. 15, n. 5, p. 3339–3353, 2016.

Zaidi, A. A.; Baldemair, R.; Tullberg, H.; Bjorkegren, H.; Sundstrom, L.; Medbo, J.; Kilinc, C.; Silva, I. D. Waveform and numerology to support 5G services and requirements. **IEEE Communications Magazine**, IEEE, v. 54, n. 11, p. 90–98, 2016.

Zappone, A.; Björnson, E.; Sanguinetti, L.; Jorswieck, E. A framework for globally optimal energy-efficient resource allocation in wireless networks. In: IEEE. **Acoustics, Speech and Signal Processing (ICASSP), 2016 IEEE International Conference on**. [S.l.], 2016. p. 3616–3620.

Zhang, Y.; Zhang, D.; Pang, L.; Chi, M.; Li, Y.; Ren, G.; Li, J. Power optimization for massive mimo systems with hybrid energy harvesting transmitter. **IEEE Transactions on Vehicular Technology**, IEEE, v. 67, n. 10, p. 10039–10043, 2018.

Zhao, L.; Zheng, K. Cooperative energy broadcasting system with massive MIMO. **IEEE Communications Letters**, v. 20, n. 6, p. 1247–1250, 2016.

Zhao, Y.; Adve, R.; Lim, T. J. Improving amplify-and-forward relay networks: optimal power allocation versus selection. In: IEEE. **2006 IEEE International Symposium on Information Theory**. [S.l.], 2006. p. 1234–1238.